Synthesis, Crystal and Molecular Structures, and Reactions of a Benzodicobaltacyclohexene, a Thermally Derived Mononuclear *o*-Xylylene Complex, and an Unsymmetrical Phosphine-Derived Dinuclear Complex

William H. Hersh, Frederick J. Hollander, and Robert G. Bergman*

Contribution from the Department of Chemistry, University of California, Berkeley, California 94720. *Received December 27, 1982*

Abstract: Alkylation of $Na[CpCo(\mu\text{-}CO)]_2$ (Cp = η^5-cyclopentadienyl) with α,α'-dibromo-*o*-xylene gives bis(μ-carbonyl)-(μ-*o*-xylylene)bis[(η^5-cyclopentadienyl)cobalt](*Co-Co*) (**1**), the first dimetallacyclohexene. The X-ray crystal structure of the derivative analogue **8** having η^5-methylcyclopentadienyl rings was solved (2371 reflections; R = 2.64%; space group $P\bar{1}$; a = 9.1045 (11), b = 9.5465 (13), c = 11.8147 (16) Å; α = 83.730 (11)°; β = 81.414 (10)°, γ = 63.392 (10)°; Z = 2, d_{calcd} = 1.598 g/cm^3) and shows a six-membered ring containing two cobalt atoms with a Co-Co "single bond" length of 2.438 Å; the dimetallacycle ring adopts a boat conformation with a folding angle of 58.5°. Compound **1** undergoes slow decomposition at room temperature in solution to give $CpCo(CO)_2$ (**10**) and the new complex (η^5-cyclopentadienyl)(η^4-*o*-xylylene)cobalt (**11**). The crystal structure of **11** (1370 reflections; R = 3.90%; space group *Pbca*; a = 7.6286 (40), b = 11.6094 (16), c = 23.7196 (24) Å; Z = 8, d_{calcd} = 1.443 g/cm^3) is that of a diene complex in which the *o*-xylylene ligand consists of a delocalized butadiene portion and a nonaromatic six-membered carbocycle. Photolysis of **1** also leads to **10** and **11** as primary products. Carbonylation of mononuclear *o*-xylylene complex **11** at 70 °C gives **10** and the CO insertion product 2-indanone (**13**). Carbonylation of **1** yields **10** and dimers **14** and **15** of free *o*-xylylene (**4**). Reactions of **1** with phosphines and phosphites (L) also give **14** and **15** as well as CpCo(CO)L (**16**), but the unstable dinuclear intermediate **17**, proposed to be $Cp_2Co_2(\mu\text{-}CO)_2(L)$, was detected in the phosphine reactions. This material can also be prepared from the dinuclear compound $[CpCo(\mu\text{-}CO)]_2$ (**3**) and phosphines. Compound **17** (L = PMe_3) decomposes via parallel first- and second-order pathways in the presence of PMe_3, while **17** (L = PPh_3) decomposes primarily via a first-order pathway in the presence of PPh_3. The X-ray crystal structure of an analogue of **17**, $(MeCp)_2Co_2(\mu\text{-}CO)_2(PPhMe_2)$ (**20**), was determined (2664 reflections; R = 2.76%; space group $P2_1/c$; a = 10.0035 (14), b = 14.0816 (13), c = 14.4761 (18) Å; β = 92.042 (11)°; Z = 4, d_{calcd} = 1.533 g/cm^3) and indicates the presence of a Co-Co "single bond" (2.416 Å); the phosphine is bound to one of the cobalt atoms, and the two carbonyls are semibridging, with the closer contacts being to the cobalt atom not bound to phosphine.

A recurrent theme in recent organometallic chemistry is the hypothesis that metallacycles—particularly those that are saturated—are key intermediates in a variety of reactions. This proposal has been well documented and accepted for reactions as diverse as olefin metathesis,[1] alkene dimerization,[2] metal-catalyzed rearrangements of strained organic rings,[3] and most recently C-H activation.[4] In addition, some recent and perhaps more speculative suggestions have been made proposing that metallacycles are also intermediates in Ziegler-Natta polymerization[5] and the Fischer-Tropsch reaction.[6]

In recent years organometallic chemists increasingly have turned their attention toward the study of dinuclear systems, partly to determine whether or not reactions occurring at two metal centers will differ fundamentally from those occurring at only one. Dimetallacycles, that is metallacycles containing two metals in the ring, are ideal systems with which to examine this question, since the reactive organic moiety is already attached to the two metal centers, and comparisons to the more numerous mononuclear metallacycles may be made. Two points of reference in such comparisons are the number of carbons in the ring and the ring size itself. While mononuclear "metallacycles" containing 1-5 methylene units are well known, such is not the case for dinuclear systems: several kinetically stable three-membered dimetallacycles containing a single methylene have been examined,[7] and one similarly stable five-membered dicobalt system containing a trimethylene bridge has been found.[8] Saturated four-[9] and six-membered[10] dimetallacycles have until recently[8] been virtually unknown. The six-membered system is of particular interest, since

Scheme I

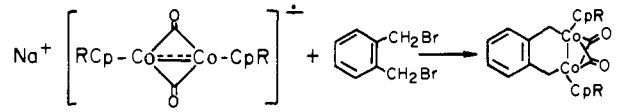

2 (R = H)
7 (R = CH3)
1 (R = H)
8 (R = CH3)

(1) (a) Katz, T. J. In "Advances in Organometallic Chemistry"; Stone, F. G. A., West, R., Eds.; Academic Press: New York, 1977; Vol. 16, p 283-317. (b) Grubbs, R. H. In "Progress in Inorganic Chemistry"; Lippard, S. J., Ed.; Wiley: New York, 1978; Vol. 24, p 1-50.

(2) (a) Datta, S.; Fischer, M. B.; Wreford, S. S. *J. Organomet. Chem.* **1980**, *188*, 353-366. (b) McLain, S. J.; Sancho, J.; Schrock, R. R. *J. Am. Chem. Soc.* **1980**, *102*, 5610-5618. (c) Fellmann, J. D.; Schrock, R. R.; Rupprecht, G. A. *Ibid.* **1981**, *103*, 5752-5758.

(3) (a) Bishop, K. C., III *Chem. Rev.* **1976**, *76*, 461-86. (b) Halpern, J. In "Organic Synthesis via Metal Carbonyls"; Wender, I., Pino, P., Eds.; Wiley: New York, 1977; Vol. II, p 705-730.

(4) (a) Chappell, S. D.; Cole-Hamilton, D. J. *J. Chem. Soc., Chem. Commun.* **1980**, 238-239. (b) Chapell, S. D.; Cole-Hamilton, D. J. *Ibid.* **1981**, 319-320. (c) DiCosino, R.; Moore, S. S.; Sowinski, A. F.; Whitesides, G. M. *J. Am. Chem. Soc.* **1982**, *104*, 124-133 and references cited therein.

(5) (a) Ivin, K. J.; Rooney, J. J.; Stewart, C. D.; Green, M. L. H.; Mahtab, R. *J. Chem. Soc., Chem. Commun.* **1978**, 604-606. (b) Fellmann, J. D.; Rupprecht, G. A.; Schrock, R. R. *J. Am. Chem. Soc.* **1979**, *101*, 5099-5101.

(6) Hugues, F.; Besson, B.; Bussiere, P.; Dalmon, J. A.; Basset, J. M.; Olivier, D. *Nouv. J. Chim.* **1981**, *5*, 207-210.

(7) Herrmann, W. A. In "Advances in Organometallic Chemistry"; Stone, F. G. A., West, R., Eds.; Academic Press: New York, 1982; Vol. 20, p 159-263.

(8) (a) Theopold, K. H.; Bergman, R. G. *J. Am. Chem. Soc.* **1980**, *102*, 5694-5695. (b) Theopold, K. H.; Bergman, R. G. *Organometallics* **1982**, *1*, 1571-1579. Note **Added in Proof**: Very recently two diosmacyclobutanes have been reported: (c) Motyl, K. M.; Norton, J. R.; Schauer, C. K.; Anderson, O. P. *J. Am. Chem. Soc.* **1982**, *104*, 7325-7326. (b) Burke, M. R.; Takats, J.; Grevels, F.-W.; Reuvers, J. G. A. *Ibid.* **1983**, *105*, 4092-4093.

(9) There are a few examples of unsaturated four-membered dimetallacycles. See, e.g.: (a) Johnson, B. F. G.; Kelland, J. W.; Lewis, J.; Rehani, S. K. *J. Organomet. Chem.* **1976**, *113*, C42-C44. (b) Smart, L. E.; Browning, J.; Green, M.; Laguna, A.; Spencer, J. L.; Stone, F. G. A. *J. Chem. Soc., Dalton Trans.* **1977**, 1777-1785. (c) Rausch, M. D.; Gastinger, R. G.; Gardner, S. A.; Brown, R. K.; Wood, J. S. *J. Am. Chem. Soc.* **1977**, *99*, 7870-7876. (d) Dickson, R. S.; Mok, C.; Pain, G. *J. Organomet. Chem.* **1979**, *166*, 385-402. (e) Boag, N. M.; Green, M.; Stone, F. G. A. *J. Chem. Soc., Chem. Commun.* **1980**, 1281-1282.

(10) Known unsaturated six-membered dimetallacycles are mostly of the type formed by oligomerization of alkynes. See, for example, ref 9b and the following: (a) Knox, S. A. R.; Stansfield, R. F. D.; Stone, F. G. A. *J. Chem. Soc., Chem. Commun.* **1978**, 221-223. (b) Slater, S.; Muetterties, E. L. *Inorg. Chem.* **1981**, *20*, 946-947.

0002-7863/83/1505-5834$01.50/0

like the five-membered mononuclear metallacycle it might model intermediates found in olefin dimerization. However, the only known dimetallacyclohexane[8] is far less stable than the analogous dimetallacyclopentane, decomposing, presumably via facile β-hydride elimination, below room temperature to give a mixture of butenes.[11] It is immediately apparent, then, that six-membered dimetallacycles may have little in common, in terms of stability, with six-membered mononuclear metallacycles, since in at least one series these were shown to be of comparable stability to the five-membered systems.[12]

In order to examine a six-membered dimetallacycle that would be at least partially saturated yet still be kinetically stable, we decided to prepare a system in which β-elimination would not be possible. In this paper we describe the successful achievement of this goal, in which benzannulation of the ring has resulted in the synthesis of the first dimetallacyclohexene.[13] We report here in full the chemistry and X-ray crystal structures both of this compound and of two of its unusual decomposition products; in an accompanying paper[14] we describe the full mechanistic details of these novel transformations.

Results and Discussion

Synthesis and Structure of Benzodicobaltacyclohexene 1. The metallacycle synthesis used was based on that previously employed to prepare a variety of bis(μ-carbonyl)bis[(η^5-cyclopentadienyl)cobalt](*Co–Co*) metallacycles.[8] Thus, addition of THF to a 1.5:1 mixture of solid α,α'-dibromo-*o*-xylene and the dinuclear radical anion[15] **2** gave the neutral compound [CpCo(μ-CO)]$_2$ (**3**) and metallacycle **1** (Scheme I). Decomposition

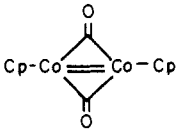

3

of **3** under the reaction conditions used facilitated the isolation of **1** as an air-stable dark green powder in 40% yield. Support for the structure shown for **1** was obtained by comparison of the IR and NMR spectral data to those of other known dialkyl dicobalt compounds.[8] Thus, the strong IR band at 1811 cm^{-1}, singlets in the ^{1}H NMR due to the methylene and cyclopentadienyl protons, and the aromatic resonances that are typical of *o*-dialkylbenzenes and the upfield shift of the methylene carbons in the ^{13}C NMR all pointed toward a symmetrical dimetallacycle containing bridging carbonyl ligands.

Closer examination of the ^{1}H NMR signal due to the methylene protons at δ 1.57 showed it to be significantly broader, at room temperature, than that due to the cyclopentadienyl protons. Gradual cooling of the sample in the NMR probe confirmed this observation: broadening of the methylene signal was followed by its virtual disappearance between −30 and −50 °C, and continued cooling to −80 °C gave rise to two new doublets at δ 2.71 and 0.22 (J = 6 Hz), each integrating as two protons relative to the unchanged aromatic and cyclopentadienyl signals. Assuming a coalescence temperature of −40 ± 10 °C, $\Delta G^{\ddagger}$(−40 °C) = 10.2 ± 0.5 kcal/mol for the exchange process. A process consistent with this is shown in Scheme II, in which the ground-state conformation of **1** is a strongly bent boat conformation; ring flipping may then proceed via the planar transition state in which all four methylene protons are equivalent as required. Although **1** is formally a cyclohexene-type ring, the ring inversion process with

Scheme II

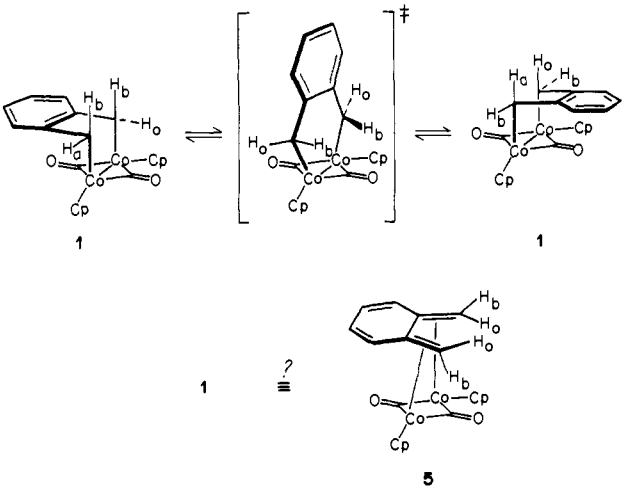

its 10 kcal/mol barrier does not appear to be comparable to that seen in cyclohexene itself: eclipsing interactions in cyclohexene that are not present in **1** (due to the two "homoallylic" cobalts) result in a boat transition state of the six-carbon ring that is about 5 kcal/mol higher than the half-chair ground state.[16]

A significant worry in proposing that the ground-state conformation of **1** is a boat cyclohexene ring is that in the extreme such a conformation might more accurately be described as a π-complex in which the diene *o*-xylylene (**4**) is bound to the

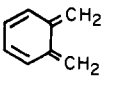

4

dicobalt moiety, as depicted by **5** in Scheme II. Indeed the large chemical shift difference (2.5 ppm) between the inequivalent protons in the frozen-out form of **1** at −80 °C suggests the sharp endo–exo environment separation that a diene would provide. However, the diene formulation would require, on the basis of the effective atomic number rule, that there be no cobalt–cobalt bond. In fact an X-ray structure of the dinuclear monocarbonyl rhodium complex (μ-carbonyl)(μ-η^4-cyclohexadiene)bis[(η^5-indenyl)rhodium] (**6**) shows that a metal–metal bond is present and that the diene is bound in π, rather than σ, fashion.[17] Thus the assumption of a metallacyclic structure for dicarbonyl complex **1** would allow a correlation between the number of carbonyls and the mode of ligand binding to exist for dimetallacycle **1** and diene complex **6**.

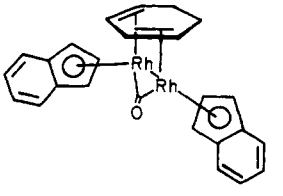

6

Spectroscopic evidence that the ligand in **1** is σ-bound may be obtained from the NMR coupling constants. In the ^{1}H NMR a geminal coupling constant of J_{HH} = 6 Hz was observed. While this is fairly small,[18] it is significantly larger than the 1.5-Hz geminal coupling constants observed in two related mononuclear cyclopentadienylcobalt diene complexes (see below). Further

(11) Theopold, K. H.; Hersh, W. H.; Bergman, R. G. *Isr. J. Chem.* **1982**, *22*, 27–29.
(12) McDermott, J. X.; White, J. F.; Whitesides, G. M. *J. Am. Chem. Soc.* **1976**, *98*, 6521–6528.
(13) Part of the results described here have been reported in preliminary form: Hersh, W. H.; Bergman, R. G. *J. Am. Chem. Soc.* **1981**, *103*, 6992–6994.
(14) Hersh, W. H.; Bergman, R. G. *J. Am. Chem. Soc.*, following article this issue.
(15) Schore, N. E.; Ilenda, C. S.; Bergman, R. G. *J. Am. Chem. Soc.* **1977**, *99*, 1781–1787.
(16) (a) Anet, F. A. L.; Haq, M. Z. *J. Am. Chem. Soc.* **1965**, *87*, 3147–3150. (b) Dashevsky, V. G.; Lugovskoy, A. A. *J. Mol. Struct.* **1972**, *12*, 39–43.
(17) Al-Obaidi, Y. N.; Green, M.; White, N. D.; Bassett, J.-M.; Welch, A. J. *J. Chem. Soc., Chem. Commun.* **1981**, 494–496.
(18) Williams, D. H.; Fleming, I. "Spectroscopic Methods in Organic Chemistry", 2nd ed.; McGraw-Hill: London, 1973; Chapter 3.

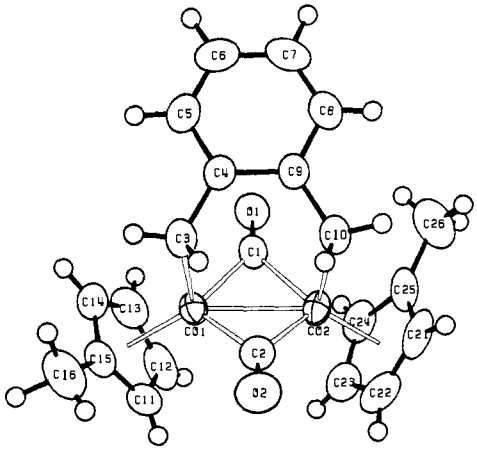

Figure 1. ORTEP drawing of one molecule of **8** with the labeling scheme. The hydrogens are shown as arbitrary small spheres for clarity. All other atoms are represented by 50% probability ellipsoids. The A hydrogens of C(3) and C(10) are endo to the metallacycle ring, the B hydrogens exo.

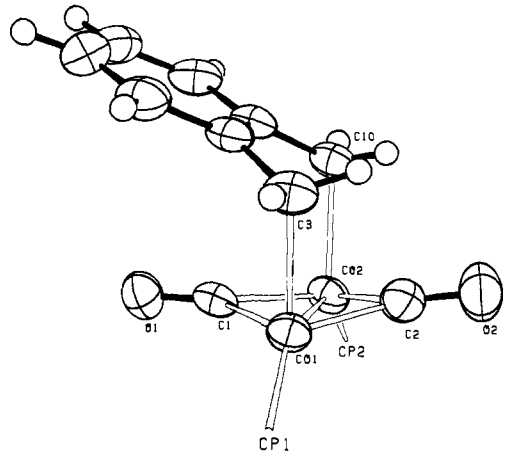

Figure 2. ORTEP drawing of **8** showing the geometry about the Co(1)–Co(2) bond. The A hydrogens of C(3) and C(10) are to the right of their respective carbons, as viewed, while the B hydrogens point toward and away from the viewer, respectively.

evidence is provided by the methylene C–H coupling constant J_{CH} = 139 Hz that was observed in the ^{13}C NMR; this value is similar to that seen (135 Hz) in the fully saturated five-membered ring dicobalt complex $Cp(\mu\text{-}CO)Co[CH(CH_3)(CH_2)_2]Co(\mu\text{-}CO)Cp$, in which the three-carbon bridge cannot be bound in π fashion.[19] In addition, these values are significantly smaller than the methylene C–H coupling constants in the diene complexes mentioned above, where J_{CH} = 157 Hz (see below). Thus, the coupling constants provide strong support for a metallacyclic structure in which the hybridization at the methylene carbons is much closer to sp^3 than sp^2.

In order to provide definitive evidence for the mode of bonding of the *o*-xylylene moiety in **1**, an X-ray structure determination was required. Unfortunately, only thin needles of **1**, quite unsuited for X-ray diffraction purposes, could be obtained. An analogue of **1** was therefore prepared from the methyl derivative $Na[(\eta^5\text{-}MeCp)_2Co_2(\mu\text{-}CO)_2]$ (**7**) and α,α'-dibromo-*o*-xylene, giving $(\eta^5\text{-}MeCp)_2Co_2(\mu\text{-}CO)_2(\mu\text{-}o\text{-}xylylene)$ (**8**) (cf. Scheme I) in 32% yield. Since both the chemistry and NMR behavior of **8** are similar to those of **1**, we assume that the structures do not differ significantly. In this case, crystals suitable for X-ray diffraction could in fact be grown.

The crystal structure of **8** consists of well-separated molecules with no unusual intermolecular contacts. Figure 1 shows an ORTEP drawing of one molecule with the labeling scheme, viewed roughly normal to the *o*-xylylene plane, while Figure 2 shows a view along the Co–Co bond (the MeCp rings have been omitted for clarity). Selected distances and angles are listed in Table I.

As expected, the gross structure is that shown in Scheme I. The geometry about the cobalt atoms places the methylene carbons C(3) and C(10), the centroids of the MeCp rings, and the two cobalts themselves in very nearly the same plane. The Co(1)–Co(2)–C(1) and Co(1)–Co(2)–C(2) planes containing the carbonyl carbons are roughly perpendicular to that plane; although both are bent somewhat away from the MeCp rings. The dihedral angles between them and the Co(1)–Co(2)–C(3)–C(10) plane are 86.5° and 78.4° respectively. Both MeCp rings are practically planar (±0.008 Å), and are tilted about 2° with respect to the Co–Cp (centroid) vector such that the methyl carbons are closer to the rest of the molecule. The folding angle of the dimetallacycle ring (the angle between the Co(1)–Co(2)–C(3)–C(10) plane and the C(3)–C(10)–C(4)–C(9) plane) is 58.5°. The two ligating methylenes lie slightly but significantly out of the plane of the phenyl ring in the direction toward the cobalt atoms. The deviation from planarity of the six-membered carbon ring is only ±0.003 (3) Å, while C(3) and C(10) lie 0.115 (2) and 0.110 (2) Å below this plane.

(19) Yang, G. K.; Bergman, R. G. *J. Am. Chem. Soc.*, in press.

Scheme III

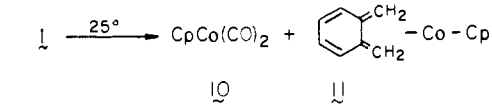

10 **11**

The key question answered by the X-ray structure is the mode of bonding of the *o*-xylylene ligand. Clearly the folding angle of roughly 60° argues against π-bonding. In addition, the Co(1)–C(4) and Co(2)–C(9) distances average 2.98 Å and are clearly nonbonding (the bonding Co(1)–C(3) and Co(2)–C(10) distances are both 2.085 (2) Å). Final definitive evidence is provided by the locations of the methylene hydrogens of **8**, which are completely consistent with sp^3 hybridization. In closing our discussion of the structure of **8**, it is worth noting that none of the bond lengths or angles indicates any strain in the ring, and the folding of the metallacycle ring appears simply to be a consequence of the differences in bond lengths and angles about the cobalt atoms relative to those that would be found about carbon in cyclohexene itself.

Thermal Decomposition of 1. Having established the solution and solid-state structures of **1** and **8**, we now turn our attention to reactions of these compounds. Solutions of **1** that were allowed to stand at room temperature (in benzene) slowly changed color from dark green to deep red over the course of about 1 day. Monitoring this decomposition by IR showed that disappearance of the major band of **1** at 1811 cm^{-1} was accompanied only by the appearance of two carbonyl bands at 2018 and 1960 cm^{-1}, both due to $CpCo(CO)_2$ (**10**). Monitoring the reaction in C_6D_6 by ^1H NMR showed disappearance of **1** with concomitant quantitative formation of two cyclopentadienyl singlets of equal intensity, one of which was due to $CpCo(CO)_2$, new doublets at δ 2.65 and –0.54 (J = 1.4 Hz), and a new aromatic AA′BB′ system centered at 7.22. Repetition of this decomposition on a preparative scale resulted in isolation of the new material in 88% yield, as slightly air-sensitive red-black crystals. On the basis of the analytical and spectroscopic data the compound was identified as the previously unknown mononuclear *o*-xylylene complex **11** (Scheme III).

Just as application of the effective atomic number rule predicted that **1** was a σ-complex, we expected that **11** would be a π-complex. Several mononuclear *o*-xylylene complexes are in fact known,[4a,b,20] but only those in the iron group[4b,20a] and possibly a

(20) (a) Roth, W. R.; Meier, J. D. *Tetrahedron Lett.* **1967**, 2053–2058. (b) Lappert, M. F.; Martin, T. R.; Atwood, J. L.; Hunter, W. E. *J. Chem. Soc., Chem. Commun.* **1980**, 476–477. (c) Lappert, M. F.; Martin, T. R.; Milne, C. R. C.; Atwood, J. L.; Hunter, W. E.; Pentilla, R. E. *J. Organomet. Chem.* **1980**, *192*, C35–C38. (d) Lappert, M. F.; Raston, C. L.; Rowbottom, G. L.; White, A. H. *J. Chem. Soc., Chem. Commun.* **1981**, 6–8. (e) Lappert, M. F.; Raston, C. L.; Shelton, B. W.; White, A. H. *Ibid.* **1981**, 485–486.

Table I. Selected Distances (Å) and Angles (deg)[a] in 8

Co(1)-Co(2)	2.438 (1)		
Co(1)-C(1)	1.893 (2)	Co(2)-C(1)	1.909 (2)
Co(1)-C(2)	1.883 (2)	Co(2)-C(2)	1.874 (2)
Co(1)-C(3)	2.085 (2)	Co(2)-C(10)	2.085 (2)
Co(1)-C(11)	2.114 (2)	Co(2)-C(21)	2.060 (2)
Co(1)-C(12)	2.130 (2)	Co(2)-C(22)	2.122 (2)
Co(1)-C(13)	2.123 (2)	Co(2)-C(23)	2.135 (2)
Co(1)-C(14)	2.074 (2)	Co(2)-C(24)	2.127 (2)
Co(1)-C(15)	2.091 (2)	Co(2)-C(25)	2.095 (2)
Co(1)-Cp(1)	1.738[b]	Co(2)-Cp(2)	1.738[b]
C(11)-C(12)	1.408 (4)	C(21)-C(22)	1.395 (4)
C(12)-C(13)	1.381 (4)	C(22)-C(23)	1.400 (3)
C(13)-C(14)	1.381 (4)	C(23)-C(24)	1.403 (3)
C(14)-C(15)	1.418 (3)	C(24)-C(25)	1.401 (3)
C(15)-C(11)	1.403 (3)	C(25)-C(21)	1.417 (4)
C(15)-C(16)	1.477 (4)	C(25)-C(26)	1.494 (4)
C(3)-C(4)	1.469 (3)	C(7)-C(8)	1.372 (3)
C(10)-C(9)	1.469 (3)	C(8)-C(9)	1.399 (3)
C(4)-C(5)	1.395 (3)	C(9)-C(4)	1.410 (3)
C(5)-C(6)	1.370 (3)	C(1)-O(1)	1.157 (2)
C(6)-C(7)	1.371 (4)	C(2)-O(2)	1.167 (2)
Co(2)-Co(1)-C(3)	96.22 (6)	Co(1)-Co(2)-C(10)	96.87 (6)
Co(2)-Co(1)-Co(1)	141.2[b]	Co(1)-Co(2)-Cp(2)	140.8[b]
C(3)-Co(1)-Cp(1)	122.4[b]	C(10)-Co(2)-Cp(2)	122.4[b]
C(3)-Co(1)-C(1)	92.14 (8)	C(10)-Co(2)-C(1)	90.92 (8)
C(3)-Co(1)-C(2)	84.48 (9)	C(10)-Co(2)-C(2)	86.51 (9)
Cp(1)-Co(1)-C(1)	124.0[b]	Cp(2)-Co(2)-C(1)	122.6[b]
Cp(1)-Co(1)-C(2)	124.9[b]	Cp(2)-Co(2)-C(2)	126.1[b]
C(1)-Co(1)-C(2)	98.61 (8)	C(1)-Co(2)-C(2)	98.38 (8)
Co(1)-C(1)-Co(2)	79.77 (8)	Co(1)-C(2)-Co(2)	80.90 (8)
Co(1)-C(1)-O(1)	140.71 (15)	Co(1)-C(2)-O(2)	138.35 (18)
Co(2)-C(1)-O(1)	139.12 (15)	Co(2)-C(2)-O(2)	140.73 (18)
Co(1)-C(3)-C(4)	112.32 (13)	Co(2)-C(10)-C(9)	113.30 (13)
Co(1)-C(3)-H3A	107.0 (12)	Co(2)-C(10)-H10A	99.7 (13)
Co(1)-C(3)-H3B	102.1 (12)	Co(2)-C(10)-H10B	107.5 (12)
C(4)-C(3)-H3A	111.6 (12)	C(9)-C(10)-H10A	115.9 (13)
C(4)-C(3)-H3B	114.6 (12)	C(9)-C(10)-H10B	109.8 (12)
H3A-C(3)-H3B	108.7 (17)	H10A-C(10)-H10B	110.0 (18)
C(3)-C(4)-C(9)	120.75 (17)	C(10)-C(9)-C(4)	120.82 (17)
C(3)-C(4)-C(5)	120.97 (18)	C(10)-C(9)-C(8)	120.85 (19)
C(9)-C(4)-C(5)	118.07 (18)	C(8)-C(9)-C(4)	118.17 (19)
C(4)-C(5)-C(6)	122.69 (22)	C(9)-C(8)-C(7)	121.78 (22)
C(5)-C(6)-C(7)	119.00 (23)	C(8)-C(7)-C(6)	120.29 (22)
C(15)-C(11)-C(12)	108.4 (2)	C(25)-C(21)-C(22)	110.0 (2)
C(11)-C(12)-C(13)	108.7 (2)	C(21)-C(22)-C(23)	106.9 (3)
C(12)-C(13)-C(14)	107.4 (2)	C(22)-C(23)-C(24)	108.3 (2)
C(13)-C(14)-C(15)	110.1 (2)	C(23)-C(24)-C(25)	109.2 (2)
C(14)-C(15)-C(11)	105.5 (2)	C(24)-C(25)-C(21)	105.6 (2)
C(14)-C(15)-C(16)	126.6 (3)	C(24)-C(25)-C(26)	126.7 (3)
C(11)-C(15)-C(16)	127.8 (3)	C(21)-C(25)-C(26)	127.6 (3)

Torsional Angles

C(3)-Co(1)-Co(2)-C(10)	-2.3
C(3)-Co(1)-Co(2)-Cp(2)	177.8
C(10)-Co(2)-Co(1)-Cp(1)	-177.2
Cp(1)-Co(1)-Co(2)-Cp(2)	2.8
C(3)-Co(1)-Cp(1)-C(14)	28.7
C(3)-Co(1)-Cp(1)-C(15)	-44.4
C(3)-Co(1)-Cp(1)-C(16)	-43.7
C(10)-Co(2)-Cp(2)-C(21)	25.1
C(10)-Co(2)-Cp(2)-C(25)	-47.6
C(10)-Co(2)-Cp(2)-C(26)	-47.6
C(5)-C(4)-C(3)-Co(1)	107.4
C(5)-C(4)-C(3)-H3A	-132.5
C(5)-C(4)-C(3)-H3B	-8.5
C(8)-C(9)-C(10)-Co(2)	-109.3
C(8)-C(9)-C(10)-H10A	136.4
C(8)-C(9)-C(10)-H10B	11.0

[a] In this and all subsequent tables, the esd's, given in parentheses right-adjusted to the least significant digit(s) shown, are calculated including the correlation terms derived from the inverted least-squares matrix. Distances and angles are uncorrected for thermal motion. [b] Cp(1) and Cp(2) are the centroids of the two methylcyclopentadienyl rings.

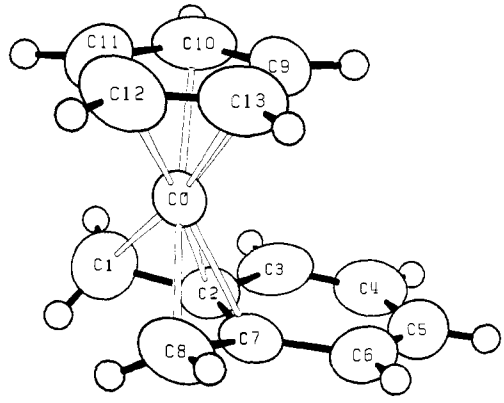

Figure 3. ORTEP drawing of **11** with the labeling scheme. The hydrogens are shown as arbitrary small spheres for clarity. The ellipsoids for all non-hydrogen atoms represent the 50% probability surface. The A hydrogens of C(1) and C(8) are to the left of their respective carbons and are endo to the C(1), C(2), C(7), C(8) unit, while the B hydrogens point away from and toward the viewer, respectively.

Table II. Selected Distances (Å) and Angles (deg)[a] in 11

Co-C(1)	2.002 (2)	C(1)-C(2)-C(3)	126.8 (3)
Co-C(2)	2.012 (2)	C(1)-C(2)-C(7)	114.7 (2)
Co-C(7)	2.007 (2)	C(3)-C(2)-C(7)	117.8 (2)
Co-C(8)	2.013 (3)	C(2)-C(3)-C(4)	121.3 (2)
Co-C(9)	2.078 (2)	C(3)-C(4)-C(5)	121.5 (3)
Co-C(10)	2.054 (3)	C(4)-C(5)-C(6)	120.9 (3)
Co-C(11)	2.030 (3)	C(5)-C(6)-C(7)	120.4 (3)
Co-C(12)	2.012 (3)	C(6)-C(7)-C(2)	118.1 (2)
Co-C(13)	2.034 (2)	C(6)-C(7)-C(8)	124.7 (2)
C(1)-C(2)	1.441 (3)	C(2)-C(7)-C(8)	116.4 (2)
C(2)-C(3)	1.414 (3)	C(2)-C(1)-H1A	114.5 (18)
C(2)-C(7)	1.437 (3)	C(2)-C(1)-H1B	107.0 (14)
C(3)-C(4)	1.326 (4)	H1A-C(1)-H1B	131.3 (23)
C(4)-C(5)	1.395 (4)	C(7)-C(8)-H8A	110.9 (16)
C(5)-C(6)	1.332 (4)	C(7)-C(8)-H8B	116.9 (17)
C(6)-C(7)	1.434 (3)	H8A-C(8)-H8B	125.4 (23)
C(7)-C(8)	1.427 (4)	C(13)-C(9)-C(10)	108.4 (3)
C(9)-C(10)	1.360 (4)	C(9)-C(10)-C(11)	109.3 (3)
C(10)-C(11)	1.387 (5)	C(10)-C(11)-C(12)	107.5 (3)
C(11)-C(12)	1.370 (5)	C(11)-C(12)-C(13)	107.7 (3)
C(12)-C(13)	1.421 (4)	C(12)-C(13)-C(9)	107.1 (3)
C(13)-C(9)	1.375 (4)		

[a] See footnote *a* in Table I.

tungsten complex,[20e] may be considered, like **11**, to be π-complexes of *o*-xylylene (**4**). The anticipated similarity in the iron group compounds and **11** in their mode of binding of *o*-xylylene is reflected in the great similarity of their ^{1}H NMR spectra. Evidence that this is indeed π-bonding is again provided by the size of the geminal proton coupling constant (1.4 Hz)[18] and by the large (relative to dinuclear metallacycle **1**) methylene C–H coupling constant of 156 Hz. The remarkably different chemical shifts of the quaternary carbons of the *o*-xylylene moieties of **1** (147.8 ppm) and **11** (92.1 ppm) also suggest that the binding modes differ substantially. In order to compare **11** with a diene complex that could not suffer possible complications arising from aromatization of the benzene ring of **4**, we prepared the parent diene complex CpCo(1,3-butadiene) (**12**).[21] The proton and carbon chemical shifts and coupling constants are in complete accord with the postulate that **11** and **12** are isostructural.

Because **1** and **11** are the only pair of related mono- and dinuclear complexes of *o*-xylylene (**4**) and no X-ray studies on the mononuclear *o*-xylylene π-complexes had been published, we undertook such a study of **11**. The compound crystallized as distinct molecules separated by normal van der Waals contact distances. Figure 3 shows an ORTEP drawing of the molecule with the labeling scheme, viewed from the "side". Selected distances

(21) (a) Pruett, R. L.; Myers, W. R. U.S. Patent 3 159 659, 1964; *Chem. Abstr.* **1965**, *62*, 7800g. (b) Yasufuku, K.; Yamazaki, H. *Org. Mass. Spectrom.* **1970**, *3*, 23–29.

and angles are listed in Table II.

Once again, the overall structure is the expected one, in which an *o*-xylylene ligand is bound via the exocyclic double bonds to a CpCo group. The amplitudes of thermal vibration in the structure are all somewhat large but still reasonable (maximum rms amplitudes are 0.36 and 0.43 Å for *o*-xylylene and cyclopentadienyl moieties). Thus, for instance, although the cyclopentadienyl ring is normal, the C–C distances are apparently shortened by systematic effects of the concerted thermal motion. Since the molecule possesses a pseudomirror plane bisecting both the cyclopentadienyl and *o*-xylylene ligands, advantage will be taken of this chemical equivalence of the two halves of the molecule in examining the bond lengths. For instance, although there must also be systematic thermal effects on the Co–C(Cp) distances, it is clear that there is an additional, real, lengthening of Co–C(9) compared to Co–C(10) and Co–C(13) and that these are also slightly longer than Co–C(11) and Co–C(12). Hence the cyclopentadienyl ring is "slipped" toward the benzene ring.

The cyclopentadienyl ligand, the six-carbon ring, and the butadiene fragment are each very close to being planar. The two groups bound to cobalt, that is the cyclopentadienyl ring and the butadiene fragment, are tilted at an angle of 13.5° to each other such that the methylene carbons C(1) and C(8) are closer to the cyclopentadienyl ring than are the quaternary carbons C(2) and C(7). However, the six-carbon plane is bent back up toward the cyclopentadienyl ring so that it forms an angle of 171.6° with the butadiene plane. Interestingly, the phenyl plane in **8** is also bent with respect to the corresponding C(3)–C(4)–C(9)–C(10) plane (Figures 1 and 2) in the same sense–that is toward the cobalts—but to the somewhat lesser extent of 175.0°.

In considering the bonding of the *o*-xylylene ligand to the cobalt, all four Co–C(xylylene) distances are essentially equal (2.009 ± 0.003 Å) and are also significantly shorter than the Co–C(Cp) distances (2.04 ± 0.01 Å). The *o*-xylylene ligand itself consists of a well-delocalized butadiene portion with an average C–C bond distance of 1.435 ± 0.004 Å and a six-carbon ring showing clear bond length alternation and partial loss of aromaticity. This contrasts sharply with the complete lack of bond alternation in the six-carbon ring in the dinuclear *o*-xylylene complex **8**. The methylene groups themselves are twisted with respect to the butadiene plane and are slightly pyramidal, but they are clearly not tetrahedral. Similar twisting and pyramidalization have both been observed by others,[22] but only in diene complexes that were substituted at the methylene carbons. These effects result here in a decrease in the steric interaction between the two endo hydrogens H1A and H8A—which still nevertheless are separated only by 1.8 Å—and presumably an increase in the bonding interaction between the cobalt and the methylene p orbitals.[22b] In summary, the structure is in complete accord with a bonding description in which the *o*-xylylene is π-bound as a diene, rather than σ-bound as a metallacyclopentene.

Photochemical Decomposition of 1. In an attempt to prepare a dinuclear π-complex of *o*-xylylene isoelectronic (and basically isostructural) to the (cyclohexadiene)rhodium complex **6**, we briefly examined the photochemistry of the benzodimetallacyclohexene **1**, since the loss of one carbonyl would in principle give the desired compound. In practice, irradiation of **1** in C_6D_6 solution for 1 h at less than 13 °C resulted in about 80% decomposition of **1**; very little thermal decomposition would have been expected in that amount of time. A complex mixture of products was obtained: of the eight cyclopentadienyl peaks observed in the ^1H NMR, four could be assigned to $CpCo(CO)_2$ (**10**), mononuclear *o*-xylylene complex **11**, $[CpCo(CO)]_3$, and unreacted **1**, together accounting for just over 50% of the total intensity. Continued photolysis led to the formation of one major *o*-xylylene-containing organometallic product (see Experimental Section for details), but difficulties in successfully scaling up the reaction prevented its isolation. Nevertheless, information concerning the origin of this product and its possible structure was

Scheme IV

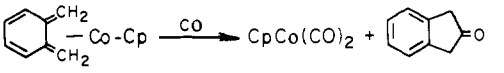

11 10 13

Scheme V

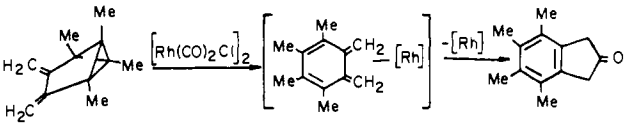

Scheme VI

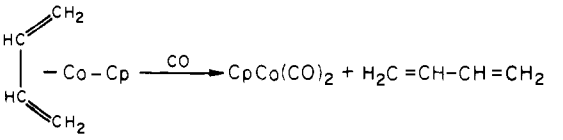

12

obtained from a control experiment: irradiation of a 1:1 mixture of $CpCo(CO)_2$ and mononuclear *o*-xylylene complex **11** gave a product mixture similar to that obtained by direct photolysis of **1**. Thus, the likely primary photoreaction of **1** is not loss of CO, but rather cleavage into **10** and **11**. The complex mixture probably results from CO loss from **10** to give CpCoCO, which may than coordinate to the uncomplexed diene portion of **11**. This type of chemistry has been observed for the photolytic reaction between $Fe(CO)_5$ and $Fe(CO)_3(\pi$-*o*-xylylene), [23] where a mixture of three dinuclear *o*-xylylene complexes was obtained in which metal bonding to both exo- and endocyclic π-bonds was suggested. We presume that the major product obtained from photolysis of **1** is likely to be analogous to one of these compounds, rather than to dinuclear rhodium complex **6** as was desired. It is nonetheless of interest that the thermal and photochemical behavior of **1** may be similar and that neither apparently results in overall CO loss.

Reaction of 1 and 11 with CO. One of our primary goals in seeking to examine the chemistry of a six-membered dimetallacycle was to study the carbonylation of such a species. Of the other dicobalt species for which this reaction had been examined, a dimethyl dicobalt compound ($Cp_2Co_2(\mu$-$CO)_2Me_2$) gave rise to the double CO insertion product acetone at room temperature,[24] while dimetallacycle **9** gave a mononuclear alkyl acyl complex that had undergone only a single insertion, at 56 °C.[8]

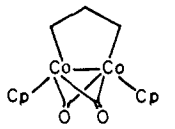

9

Reaction of mononuclear *o*-xylylene complex **11** with carbon monoxide (6 atm) occurred slowly at 70 °C in C_6D_{12} solution. After 2 days, complete conversion of **11** to $CpCo(CO)_2$ and the CO insertion product 2-indanone (**13**) had occurred (Scheme IV). To our knowledge, this reaction represents the only example of a purely thermal CO insertion into an isolable diene complex. The analogous iron *o*-xylylene complex only undergoes such an insertion with the aid of a strong Lewis acid catalyst;[25] a transient (*o*-xylylene)rhodium complex may be responsible for the carbonylation shown in Scheme V.[26] In an effor to determine whether the

(22) (a) Eiss, R. *Inorg. Chem.* **1970**, *9*, 1650–1655. (b) Wakatsuki, Y.; Aoki, K.; Yamazaki, H. *J. Chem. Soc., Dalton Trans.* **1982**, 89–94.

(23) Victor, R.; Ben-Shoshan, R. *J. Organomet. Chem.* **1974**, *80*, C1–C4.

(24) Schore, N. E.; Ilenda, C.; Bergman, R. G. *J. Am. Chem. Soc.* **1976**, *98*, 7436–7438.

(25) Johnson, B. F. G.; Lewis, J.; Thompson, D. J. *Tetrahedron Lett.* **1974**, 3789–3790.

(26) Heldeweg, R. F.; Hogween, H. *J. Am. Chem. Soc.* **1976**, *98*, 6040–6042.

Scheme VII

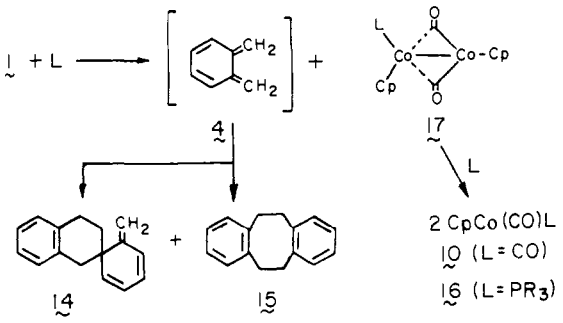

Scheme VIII

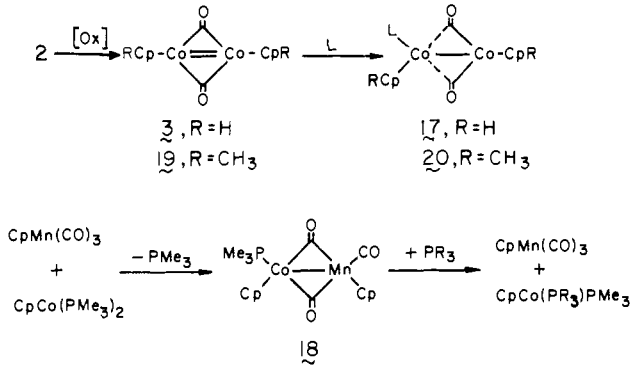

carbonylation of **11** might be unique due to the CpCo moiety, carbonylation of CpCo(1,3-butadiene) (**12**) was attempted. However, under conditions similar to those described for the reaction of **11**, as shown in Scheme VI only free butadiene and $CpCo(CO)_2$ were observed; there was no evidence to suggest that any CO insertion had occurred.

In contrast to the slow reaction of **11** with CO, carbonylation of dimetallacycle **1** gave rise to a relatively fast reaction at room temperature, in which a color change from dark green to deep red-orange was complete after 15 min under only 2 atm of CO. Also in contrast to the reaction of **11**, there was no evidence of any CO insertion; rather, the only organic products observed were dimers **14** and **15** of *o*-xylylene (Scheme VII), formed in quantitative yield along with $CpCo(CO)_2$. Phosphines and phosphites give rise to a similar reaction, leading to **14**, **15**, and **16** as the final products.

Use of bis(diphenylphosphino)ethane (diphos) as the phosphine reactant allowed **14** and **15** to be chromatographically separated from both excess phosphine and the corresponding diphos adduct **16**; in addition another material presumed to be the chelated complex CpCo(diphos) (see Experimental Section for details) was also formed. The organic products were isolated in 56% yield as a 95:5 mixture of **14**/**15** and were identified by comparison with the known NMR spectra.[27] The observed ratio is consistent with that expected for the room temperature dimerization of free *o*-xylylene (**4**) itself: spiro dimer **14** predominates at low temperatures (<0 °C) while dibenzocyclooctadiene **15** is favored at higher temperatures.[27] Thus, the reactions of **1** with dative ligands appear to involve loss of the ligand **4** as a free diene before it can be transformed at the metal center, in contrast to the reaction observed for **11**.

Reactions of 1 with Phosphines. Because the ligand-induced loss of *o*-xylylene from dimetallacycle **1** represented a dinuclear elimination reaction, we initiated a closer examination of this process. We assumed that the CO and phosphine reactions proceeded via similar pathways and for convenience therefore chose to study the phosphine chemistry. Monitoring the reaction of **1** with 0.5 M triphenylphosphine in benzene by IR revealed the presence of an unstable intermediate having a single carbonyl absorption at 1758 cm^{-1}. Disappearance of this band (and that due to the starting material at 1811 cm^{-1}) was accompanied by the appearance of the band at 1926 cm^{-1} due to the final product **16** (L = PPh_3). Monitoring the reaction by ^1H NMR also revealed the presence of the intermediate, as indicated by a broad peak in the cyclopentadienyl region of the spectrum. As in the IR, this signal was most easily observed in concentrated PPh_3 solutions, the maximum being 25% of the total cyclopentadienyl intensity after a few minutes reaction with 1.0 M PPh_3.

Reactions of **1** with more nucleophilic alkyl phosphines were more striking: rapid disappearance of the IR band due to **1** was accompanied by formation of a single carbonyl band at about 1750 cm^{-1} with PPh_2Me, $PPhMe_2$, and PEt_3. This band was observed to decay slowly with formation of the final band due to **16**. Using a single equivalent of PEt_3 in toluene-d_8, examination of the reaction by ^1H NMR showed that disappearance of **1** and formation of the intermediate was accompanied by immediate formation of dimers **14** and **15** in about 85% yield. The intermediate exhibited cyclopentadienyl peaks of equal intensity at δ 4.82 and 4.65 and signals due to one bound phosphine. Similar NMR results were obtained with PPh_2Me, $PPhMe_2$, and PMe_3; in addition, for $PPhMe_2$ and PMe_3 the higher field cyclopentadienyl signal was a poorly resolved doublet with $J_{PH} \approx 0.5$ Hz. At this point it became clear that the observed broad singlet in the PPh_3 reaction was probably due to a fluxional process, given the structural similarity in all of the intermediates suggested by the IR band at about 1750 cm^{-1} that each exhibited. Indeed, cooling a THF-d_8 solution of PPh_3 (0.18 M) and **1** (0.014 M) to −30 °C revealed two new singlets in a 1:1 ratio at δ 4.78 and 4.65; warming to room temperature resulted in gradual coalescence and a slight upfield shift to give a broad singlet at δ 4.69, before this material was transformed to **16**. Estimating the coalescence temperature to be 10 ± 5 °C gives $\Delta G^{\ddagger} = 14.2 \pm 0.3$ kcal/mol for the process that interconverts the two cyclopentadienyl resonances. This process could involve PPh_3 hopping between two cyclopentadienylcobalt moieties, or could involve exchange with free PPh_3; the latter possibility may better account for the immediate displacement of PPh_3 by PEt_3 to give the PEt_3 intermediate.

The spectral properties of the intermediate are consistent either with the structure **17** shown in Scheme VII or with a structure having symmetrically bridging CO's and a metal–metal dative bond[28] (in which the phosphine-bearing cobalt donates an electron pair to the unsaturated cobalt). We defer for the moment a discussion of the details of the structure of structure **17**, in order to describe some of its chemistry.

Alternate Synthesis of 17. The proposed structure of **17** immediately implied a second means by which it might be synthesized, since it is merely a phosphine adduct of the known dinuclear compound $[CpCo(\mu\text{-}CO)]_2$ (**3**, Scheme VIII); this material is derived from radical anion **2** by a single-electron oxidation.[15] In fact, reaction of phosphines such as PPh_3, $PPhMe_2$, or PEt_3 with **3** gave rise to an immediate color change from the deep blue-green of **3**, to the dark green characteristic of **17**, and then more slowly to the orange color of **16**. Following the reaction by both IR and NMR showed the same spectral characteristics due to **17** that were observed in the reactions of **1** with phosphines and hence provided strong support for the proposed structure of **17**. An additional piece of evidence is provided by the isoelectronic manganese cobalt complex **18** (Scheme VIII), which like **17** both undergoes a further reaction with phosphines and exhibits an unusually low-frequency IR carbonyl absorption.[29]

The reaction between **3** and phosphines to give **17** and then **16** is of particular interest in that it provides the first clear example of stepwise addition of a dative ligand to a metal–metal multiple bond. Reactions of the triple-bonded compound $[CpMo(CO)_2]_2$ are perhaps the best documented of this variety, where the gen-

(27) Errede, L. A. *J. Am. Chem. Soc.* **1961**, *83*, 949–954.

(28) (a) Deubzer, B.; Kaesz, H. D. *J. Am. Chem. Soc.* **1968**, *90*, 3276–3277. (b) Hoxmeier, R. J.; Knobler, C. B.; Kaesz, H. D. *Inorg. Chem.* **1979**, *18*, 3462–3466.

(29) (a) Leonhard, K.; Werner, H. *Angew. Chem., Int. Ed. Engl.* **1977**, *16*, 649–650. (b) Werner, H.; Juthani, B. *J. Organomet. Chem.* **1981**, *209*, 211–218. (c) An X-ray structure of **18** has been carried out; Werner, H., personal communication.

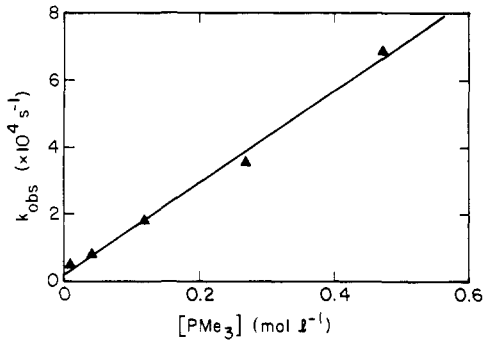

Figure 4. Plot of dependence of pseudo-first-order rate of disappearance of **17** on PMe_3 concentration.

erally observed result is addition of two dative ligands (one at each metal) with overall reduction of the bond order by two.[30] Presumably these reactions are stepwise, but to date the monosubstituted adduct analogous to **17** has not been detected. Following submission of our initial report,[13] Werner and Klingert reported similar additions of a variety of phosphines and phosphites to the rhodium complex $[(\eta^5\text{-}C_5Me_5)Rh(\mu\text{-}CO)]_2$ to give dinuclear monoadducts isoelectronic to **17**.[31] These rhodium dimers are inert to excess ligand and thus unlike **17** do not react to give mononuclear derivatives. An additional difference is that the rhodium phosphite complexes are stable, while we have not observed those of cobalt (see below). We are aware of a few other examples where such a stepwise addition has actually been detected,[32] but in two of these the overall bond order is not reduced,[32d,e] and in one of these the mechanism has been shown to be dissociative.[32e] Two systems involve hydride-bridged metal–metal double-bonded compounds, $Re_2(CO)_8(\mu\text{-}H)_2$[32b,c] and $Os_3(CO)_{10}(\mu\text{-}H)_2$.[32a] Both seem closely related to the dicobalt system, but the monosubstituted adducts were only well characterized in the osmium system, and in both ligand addition is accompanied by a bridging to terminal hydride shift.

Reaction of 17 with Phosphines. Due to the unusual nature of the dinuclear adduct **17**, a brief discussion of its decomposition to mononuclear carbonylphosphine complex **16** is warranted. First, we note that reaction of **1** with PCy_3 (Cy = cyclohexyl), $P(OMe)_3$, and $P(OPh)_3$ each led to direct formation of the corresponding mononuclear adducts **16**. We presume that the dinuclear adducts were too unstable to be detected, due to a combination of steric (PCy_3 is quite bulky) and electronic effects. Second, several reactions between **1** and PMe_3 and PPh_3 were followed kinetically. The rate of reaction of **17** with PMe_3, using a pseudo-first-order excess of PMe_3, was measured by ^1H NMR by monitoring the disappearance of **17** formed from **1** in THF-d_8 at 21.5 °C, after decomposition of **1** was complete; even in the least favorable case, less than half of the **17** formed had decomposed by this point. Clean first-order disappearance of **17** was observed, and plotting these observed first-order rate constants against [PMe_3] gave a straight line from 0.01–0.48 M PMe_3 (Figure 4). The rate law that fits these data is shown in eq 1, where $k_1 = (2.0 \pm 1.7) \times$

$$-d[\mathbf{17}]/dt = (k_1 + k_2[PMe_3])[\mathbf{17}] \qquad (1)$$

10^{-5} s^{-1} and $k_2 = (1.35 \pm 0.07) \times 10^{-3}$ M^{-1} s^{-1}. Clearly the major decomposition pathway is a bimolecular reaction between **17** and PMe_3, but a very slow first-order, PMe_3-independent, pathway also appears to be present. That a nonzero intercept is likely to exist is most clearly seen by the fact that $k_{obsd} = (4.4 \pm 0.4) \times 10^{-5}$ s^{-1} for [PMe_3] = 0.01 M, a rate that is quite close to the extrapolated decomposition rate for [PMe_3] = 0.

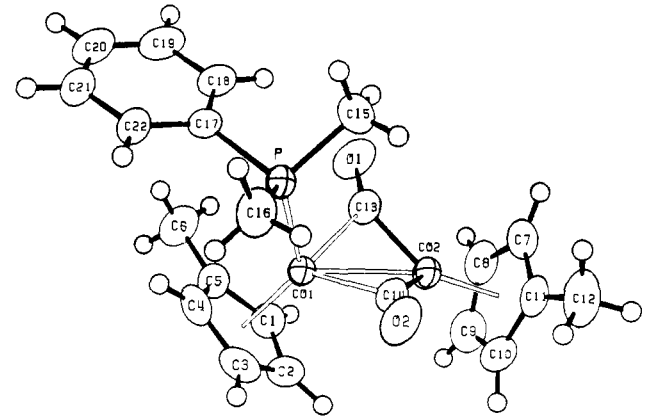

Figure 5. ORTEP drawing of **20** with the labeling scheme. The hydrogens are shown as arbitrary small spheres, while the other thermal ellipsoids are scaled to represent the 50% probability surface.

For PPh_3, monitoring the decomposition of **17** derived from **1** was somewhat less straightforward, since it was not possible to do so after complete decomposition of **1**. However, the rate of appearance of **16** was easily measured by ^1H NMR, also in THF-d_8 at 21.5 °C, and fit to a first-order plot. If the reaction follows the consecutive first-order pathway shown in eq 2, then

$$\mathbf{1} \xrightarrow{k_3} \mathbf{17} \xrightarrow{k_4} 2\,\mathbf{16} \qquad (2)$$

k_3 is simply the directly measured observed rate of decomposition of **1**,[14] while the rate of appearance of **16** can be derived analytically as a function of k_3 and k_4.[33] While the predicted rate of formation of **16** is not first order on the basis of eq 2, it was nevertheless numerically convenient to treat it as such, and experimentally the rates were indeed first order. Using the analytical rate equations for consecutive reactions[33] and the known values for k_3, k_4 was adjusted by trial and error until the calculated "first-order" rate of appearance of **16** was equal to that which was measured. The derived values of k_4 for [PPh_3] = 0.01–1.0 M ranged from 1.1×10^{-3} s^{-1} to 2.5×10^{-3} s^{-1}, with five of the six points giving $k_4 = (2.2 \pm 0.1) \times 10^{-3}$ s^{-1} over the same concentration range. Thus, for PPh_3, decomposition of **17** shows no observable dependence on [PPh_3] and is about 2 orders of magnitude more rapid than the phosphine-independent decomposition of **17** for PMe_3. Furthermore, our qualitative observations that the PMe_3 monophosphine adduct was more stable than the PPh_3 adduct and that high concentrations of PPh_3 did not lead to faster decomposition of the PPh_3 adduct are born out quantitatively. Mechanistically, we propose that for PPh_3 the major decomposition pathway is first-order fragmentation of **17** into **16** and CpCo(CO), which is then rapidly trapped by excess PPh_3 to give more **16**. The rapid fragmentation may be due to poor stabilization of the complex due to the weak Co–P bond (as evidenced by the fluctional process having $\Delta G^{\ddagger} = 14$ kcal/mol; see above), and this weakness may be caused or be exacerbated by steric hindrance. For the more nucleophilic PMe_3, a second-order pathway predominates, and presumably is due to direct attack on the nonphosphine-bearing cobalt of **17**. We presume that the stronger Co–PMe_3 bond stabilizes the ground state of **17** more than the transition state for dissociation into **16** and CpCo(CO), relative to PPh_3 (where the transition-state energies could be similar), and that this accounts for the slower first-order decomposition of **17** for PMe_3.

Structure of 17. Due to the apparently unusual nature of **17**, a more definitive characterization of this compound was desired. We discovered that the bis(methylcyclopentadienyl) monophosphine adducts were considerably more stable than the biscyclopentadienyl adducts, and thus we decided to prepare a bis-

(30) Curtis, M. D.; Klingler, R. G. *J. Organomet. Chem.* **1978**, *161*, 23–37.
(31) Werner, H.; Klingert, B. *J. Organomet. Chem.* **1982**, *233*, 365–371.
(32) (a) Shapley, J. R.; Keister, J. B.; Churchill, M. R.; De Boer, B. G. *J. Am. Chem. Soc.* **1975**, *97*, 4145–4146. (b) Andrews, M. A.; Kirtley, S. W.; Kaesz, H. D. *Inorg. Chem.* **1977**, *16*, 1556–1561. (c) Mays, M. J.; Prest, D. W.; Rauthby, P. R. *J. Chem. Soc., Chem. Commun.* **1980**, 171–173. (d) Wachter, J.; Mitschler, A.; Riess, J. G. *J. Am. Chem. Soc.* **1981**, *103*, 2121–2123. (e) Girolami, G. S.; Mainz, V. V.; Andersen, R. A.; Vollmer, S. H. *Ibid.* **1981**, *103*, 3953–3955.

(33) Moore, J. W.; Pearson, R. G. "Kinetics and Mechanism", 3rd ed.; Wiley: New York, 1981; Chapter 8.

Table III. Selected Distances (Å) and Angles (deg)[a] in **20**

Co(1)-Co(2)	2.416 (1)	Co(2)-Co(1)-P	108.02 (1)
Co(1)-P	2.191 (1)	Co(2)-Co(1)-Cp(1)	125.2[b]
Co(1)-C(1)	2.095 (2)	P-Co(1)-Cp(1)	126.8
Co(1)-C(2)	2.085 (2)	P-Co(1)-C(13)	88.45 (5)
Co(1)-C(3)	2.117 (2)	P-Co(1)-C(14)	86.68 (5)
Co(1)-C(4)	2.082 (2)	Cp(1)-Co(1)-C(13)	128.3
Co(1)-C(5)	2.127 (2)	Cp(1)-Co(1)-C(14)	127.6
Co(1)-Cp(1)	1.728[b]	C(13)-Co(1)-C(14)	85.01 (7)
Co(1)-C(13)	1.970 (2)	Co(1)-Co(2)-Cp(2)	158.9[b]
Co(1)-C(14)	2.026 (2)	Cp(2)-Co(2)-C(13)	129.1
Co(2)-C(7)	2.065 (2)	Cp(2)-Co(2)-C(14)	132.3
Co(2)-C(8)	2.082 (2)	C(13)-Co(2)-C(14)	98.00 (8)
Co(2)-C(9)	2.143 (2)	Co(1)-C(13)-Co(2)	79.71 (7)
Co(2)-C(10)	2.118 (2)	Co(1)-C(14)-Co(2)	78.45 (7)
Co(2)-C(11)	2.088 (2)	Co(1)-C(13)-O(1)	133.13 (14)
Co(2)-Cp(2)	1.724[b]	Co(1)-C(14)-O(2)	131.39 (14)
Co(2)-C(13)	1.794 (2)	Co(2)-C(13)-O(1)	146.62 (15)
Co(2)-C(14)	1.784 (2)	Co(2)-C(14)-O(2)	149.64 (15)
C(13)-O(1)	1.172 (2)	C(5)-C(1)-C(2)	108.76 (18)
C(14)-O(2)	1.173 (2)	C(1)-C(2)-C(3)	108.36 (18)
C(1)-C(2)	1.413 (3)	C(2)-C(3)-C(4)	107.02 (19)
C(2)-C(3)	1.392 (3)	C(3)-C(4)-C(5)	109.53 (18)
C(3)-C(4)	1.411 (3)	C(4)-C(5)-C(1)	106.22 (18)
C(4)-C(5)	1.410 (3)	C(4)-C(5)-C(6)	126.73 (20)
C(5)-C(1)	1.405 (3)	C(1)-C(5)-C(6)	127.01 (20)
C(5)-C(6)	1.496 (3)	C(11)-C(7)-C(8)	108.22 (19)
C(7)-C(8)	1.414 (3)	C(7)-C(8)-C(9)	108.41 (19)
C(8)-C(9)	1.393 (3)	C(8)-C(9)-C(10)	108.01 (19)
C(9)-C(10)	1.394 (3)	C(9)-C(10)-C(11)	109.13 (19)
C(10)-C(11)	1.425 (3)	C(10)-C(11)-C(7)	106.20 (18)
C(11)-C(7)	1.415 (3)	C(10)-C(11)-C(12)	126.45 (20)
C(11)-C(12)	1.488 (3)	C(7)-C(11)-C(12)	127.25 (21)
P-C(15)	1.817 (2)	Co(1)-P-C(15)	117.81 (7)
P-C(16)	1.806 (2)	Co(1)-P-C(16)	113.33 (7)
P-C(17)	1.825 (2)	Co(1)-P-C(17)	113.63 (6)
C(17)-C(18)	1.385 (3)	C(15)-P-C(16)	102.40 (9)
C(18)-C(19)	1.381 (3)	C(15)-P-C(17)	102.98 (9)
C(19)-C(20)	1.366 (3)	C(16)-P-C(17)	105.18 (9)
C(20)-C(21)	1.368 (4)	P-C(17)-C(18)	118.95 (14)
C(21)-C(22)	1.383 (3)	P-C(17)-C(22)	122.05 (15)
C(22)-C(17)	1.389 (3)	C(18)-C(17)-C(22)	118.81 (17)
		C(17)-C(18)-C(19)	120.16 (20)
		C(18)-C(19)-C(20)	120.53 (21)
		C(19)-C(20)-C(21)	120.04 (19)
		C(20)-C(21)-C(22)	120.21 (21)
		C(21)-C(22)-C(17)	120.22 (21)

Torsional Angles

Co(2)-Co(1)-P-C(15)	12.0
Co(2)-Co(1)-P-C(16)	−107.5
Co(2)-Co(1)-P-C(17)	132.5
Co(2)-Co(1)-Cp(1)-C(5)	−116.0
Cp(2)-Co(2)-Co(1)-P	−174.8
Cp(2)-Co(2)-Co(1)-Cp(1)	7.4
Co(1)-Co(2)-Cp(2)-C(11)	−138.1
Cp(2)-Co(2)-C(13)-O(1)	−17.5
Cp(2)-Co(2)-C(14)-O(2)	15.8
Co(1)-P-C(17)-C(18)	−72.1
Co(1)-P-C(17)-C(22)	102.7

[a, b] See footnotes *a* and *b*, Table I.

(methylcyclopentadienyl) adduct for X-ray analysis. Reaction of $PPhMe_2$ with neutral dimer $[(\eta^5\text{-MeCp})Co(\mu\text{-CO})]_2$ (**19**) followed by chromatography and crystallization from pentane at −40 °C gave a 30% yield of $(\eta^5\text{-MeCp})_2Co(\mu\text{-CO})_2(PPhMe_2)$ (**20**) as air-stable black-green crystals (Scheme VIII). The crystal structure consists of well-separated molecules with no short intermolecular contacts. An ORTEP drawing of the molecule with the labeling scheme is shown in Figure 5, and selected bond distances, angles, and torsional angles are compiled in Table III.

The overall structure once again is in accord with that deduced from the spectroscopic data. The metal–metal bond length of 2.416 Å is slightly shorter than that observed in bis(MeCp) dimetallacycle **8** (2.438 Å) and is likely an ordinary metal–metal single bond. Of the remaining ligands, the methylcyclopentadienyl groups exhibit no significant distortions and are bound to the cobalt atoms at distances similar to those found in **8**. The P–Co bond length of 2.191 Å also appears to be normal: values of 2.234[34] and 2.164 Å[35] have been measured in two CpCo(III) complexes, as has one of 2.173 Å in a Co(0) cluster.[36] The systematic shortening of the phenyl ring bonds toward the para-carbon (C(20)) is a systematic effect due to thermal motion and should be ignored.

One of the methyl groups on the phosphine ligand lies almost directly over the cobalt–cobalt bond, giving a Co(2)–Co(1)–P–C(15) torsion angle of only 12°. This induces additional asymmetry in the molecule, in addition to that obviously due to the phosphine being bound to a single cobalt. Thus for instance, a significant shortening (0.056 Å) of the Co(1)–C(13) bond—that is the carbonyl juxtaposed to the phenyl ring—relative to the Co(1)–C(14) bond is observed, but this difference is unlikely to persist in solution. The most obvious effects of the phosphine ligand are on the nature of the CO bonding and the positions of the methylcyclopentadienyl rings on the cobalts. Thus, the carbonyls are clearly semibridging: Co(1)–C bond distances average 2.00 Å while the Co(2)–C bonds average 1.79 Å, and the Co(1)–C–O bond angles average 132.3° while the Co(2)–C–O angles average 148.1°. A few other cobalt compounds containing semibridging carbonyls are known;[37] of these one, $[CpCo(CO)]_3$, is also a CpCo cluster, and the semibridging geometries are similar.[37a,c]

The bonding of the MeCp rings are also shifted due to the phosphine, in such a way as to allow it access. The Co(2)–Co(1)–Cp(1) angle is pushed to 125.2° compared to 141° in **8**, while the Co(1)–Co(2)–Cp(2) angle is increased to 158.9°, due to the steric interaction of the first MeCp ring. As a result, the Cp(2)–Co(2)–C(13)–C(14) moiety is almost planar: Co(2) is only 0.076 Å below the plane of the other three points. Thus in a sense the structure represents a 16-electron $(\eta^5\text{-MeCp})Co(PPhMe_2)$ moiety bound side on to $(\eta^5\text{-MeCp})Co(CO)_2$. In the time since this work was carried out, two analogous thiocarbonyl complexes have been reported,[38] and the X-ray structure of one of these, $(\eta^5\text{-Cp})_2Co_2(\mu\text{-CS})_2(PMe_3)$ (**21**), has been briefly described.[38b,c] Compound **21** is apparently isostructural to **20**; the Co–Co bond length of 2.392 Å and the semibridging thiocarbonyl Co–C bond lengths of 1.81 and 1.95 Å are similar to the values found for compound **20**.

In conclusion, we note that **20** is a saturated 34-electron cluster; as such it might be expected, and is actually observed, to have a metal–metal single bond. We mentioned above that this might be considered to be a dative bond[28] in the presence of symmetrical carbonyl bridges. However, it is apparently quite rare that ligand-induced asymmetry of the type present in **20** is mitigated in that way, the rule being rather that the carbonyls become semibridging,[39] as is observed here.

Conclusion

Our initial aim in this work was to synthesize the first kinetically stable, at least partially saturated, six-membered dimetallacycle. This has now been accomplished in the preparation of dicobaltacycle **1** (Scheme I), by the simple expedient of blocking the positions β to the two metal centers via benzannulation. This approach has, however, introduced a new set of reactions. The unusual overall result of this work is the inverse, rather than direct, relationship between the structures and chemical reactions of both

(34) Gastinger, R. G.; Rausch, M. D.; Sullivan, D. A.; Palenik, G. J. *J. Am. Chem. Soc.* **1976**, *98*, 719–723.
(35) Theopold, K. H.; Becker, P. N.; Bergman, R. G. *J. Am. Chem. Soc.* **1982**, *104*, 5250.
(36) Huie, B. T.; Knobler, C. B.; Kaesz, H. D. *J. Am. Chem. Soc.* **1978**, *100*, 3059–3071.
(37) (a) Cotton, F. A.; Jamerson, J. D. *J. Am. Chem. Soc.* **1976**, *98*, 1273–1274. (b) Colton, R.; McCormick, M. J. *Coord. Chem. Rev.* **1980**, *30*, 1–52. (c) Bailey, W. I. Jr.; Cotton, F. A.; Jamerson, J. D.; Kolthammer, B. W. S. *Inorg. Chem.* **1982**, *21*, 3131–3135.
(38) (a) Kolb, O.; Werner, H. *Angew. Chem., Int. Ed. Engl.* **1982**, *21*, 202–203. (b) Werner, H. *Coord. Chem. Rev.* **1982**, *43*, 165–168. (c) Werner, H., personal communication.
(39) Cotton, F. A. In "Progress in Inorganic Chemistry"; Lippard, S. J., Ed.; Wiley: New York, 1976; Vol. 21, p 1–28.

1 and **11**. As shown by NMR spectroscopy and X-ray diffraction, the dinuclear complex **1** has a σ-bound structure. In its chemical reactions, however, it easily releases the free π-ligand *o*-xylylene and rearranges to the π-bound complex **11**. Similarly, the mononuclear complex **11**, in which the *o*-xylylene ligand is π-bound in the ground state, leads on carbonylation to 2-indanone (**13**), a reaction that one might normally have associated with a σ-bound ligand. These observations emphasize that the structure of a molecule can be very different from the structure of the lowest energy transition state, which determines the main product formed during its chemical transformation. Thus there are often serious risks involved in attempting to predict the reactions of a molecule on the basis of its ground-state structure. In the present case, it seems clear that the lack of direct correlation between ground- and transition-state structures are a result of the closeness in energy of π- and σ-forms of *o*-xylylene, due to the energetic advantage gained from aromatization of the six-membered ring.

One question raised by this work is that of the detailed mechanism of decomposition of the dimetallacycle. An important clue would appear to be the discovery of the dinuclear monophosphine intermediate, the structure of which has now been unambiguously determined by X-ray analysis. The implication is that the elimination of *o*-xylylene is a dinuclear process. Even though no new σ-bonds are formed in this process, dinuclear eliminations of σ-bound species are rare.[40] A detailed examination of the mechanism of this elimination is presented in the accompanying paper.

Experimental Section

General. All manipulations of air-sensitive compounds were carried out either in a Vacuum Atmospheres inert atmosphere drybox under prescrubbed recirculating nitrogen or via standard vacuum line techniques. ^{1}H NMR spectra were recorded on a Varian EM-390 90-MHz spectrometer or at 200 or 250 MHz on spectrometers equipped with Cryomagnets Inc. magnets and Nicolet Model 1180 data collection systems. ^{13}C NMR spectra were recorded at 45 MHz on an instrument equipped with a Brucker superconducting magnet and a Nicolet Corp. Fourier Transform Computer package. All chemical shifts are reported relative to tetramethylsilane. Infrared spectra were obtained on a Perkin-Elmer 283 grating spectrometer with NaCl solution cells. Mass spectra (electron impact) were obtained on an AEI MS-1 spectrometer interfaced with a Finnegan 2300 data system. The field desorption mass spectrum was obtained on a Kratos MS 9 equipped with an FD source, at the U. C. Berkeley Space Sciences Laboratory. Elemental analyses were performed by the U. C. Berkeley analytical facility. Melting points were carried out in sealed tubes under nitrogen on a Thomas Hoover capillary melting point apparatus and are uncorrected.

Photolyses were carried out with an Oriel 500W high-pressure mercury lamp powered by an Oriel Corp. (Model 6128) Universal Lamp Power Supply, mounted in an Oriel focused-beam lamp housing. The reaction samples were immersed in a quartz water bath that was cooled by a 0 °C ethylene glycol/water mixture circulating through a copper coil that was in the bath. After about 2 h the bath temperature would rise to a maximum of 15 °C due to heat from the lamp.

The $CDCl_3$ used for the ^{13}C NMR spectra was dried over molecular sieves and vacuum transferred prior to use. All other deuterated solvents were purified by vacuum transfer from sodium benzophenone ketyl. Benzene, toluene, tetrahydrofuran, diethyl ether, and dimethoxyethane were distilled under nitrogen from sodium benzophenone ketyl. Hexane was purified by washing 2 times each successively with 5% nitric acid in sulfuric acid, distilled water, saturated sodium carbonate solution, and again with water, followed by drying over calcium chloride and distillation under nitrogen from *n*-butyllithium in hexane. Spectral grade *n*-pentane and methylene chloride were stirred over calcium hydride and then vacuum transferred.

Silica gel 60 was dried, using a heat gun, for several hours under dynamic vacuum. Neutral alumina II was degassed briefly at room temperature. Both were transferred under vacuum into the drybox; all the chromatography and reactions with silica and alumina were performed in the drybox by use of these two materials.

$CpCo(CO)_2$ (**10**) was prepared according to the published procedure,[41] while $(\eta^5$-MeCp)$Co(CO)_2$ was prepared in the analogous manner by using methylcyclopentadiene. The dicarbonyls used were contaminated by about 10% (by weight) of the corresponding dicyclopentadiene. Na$[(\eta^5$-Cp$)_2Co_2(CO)_2]$ (**2**) was prepared by the published procedure;[15] the crude product used contained 50–75% by weight of **2**, the remainder being THF and sodium cyclopentadienide. The amount of **2** present in a given sample was calculated by weighing the material, and then subtracting the amount of THF and NaCp present as measured by NMR analysis (CD_3CN solvent) in the presence of a known amount of ferrocene added as internal standard.

Bis(μ-carbonyl)(μ-*o*-xylylene)bis[(η^5-cyclopentadienyl)cobalt](*Co–Co*) (1). In the drybox, 30 mL of THF was added to a mixture of 2.60 g of Na[CpCo(μ-CO)]$_2$ (**2**) (4.50 mmol) and 1.81 g of α,α'-dibromo-*o*-xylene (6.84 mmol). After stirring for 5 min, the reaction flask was evacuated and the solvent rapidly removed in vacuo at room temperature. The residue was taken up in benzene and rapidly chromatographed on alumina, eluting first with hexane until a red-orange band presumed to contain $CpCo(CO)_2$ and unreacted dibromide was removed and then with benzene to remove the second (dark green) fraction. This benzene solution was quickly frozen; removal of the solvent by sublimation yielded 715 mg (39% yield) of **1** as a dark green air-stable (only as a solid) powder. Crystallization from 2:1 pentane/methylene chloride solution at −40 °C gave spectroscopically pure **1** as fine dark green needles (mp 106 °C dec); analytically pure material was obtained by crystallization from toluene/pentane, but this method was not used preparatively since crystalline material could not be reproducibly obtained: mp 109 °C dec; MS (field desorption), *m/e* 408 (M$^+$); IR (benzene) 1855 (w), 1811 (s) cm^{-1}; ^{1}H NMR (THF-d_8, 22 °C) δ 6.81, 6.71 (AA′BB′, 4 H), 5.10 (s, 10 H), 1.57 (s, 4 H); ^{1}H NMR (THF-d_8, −80 °C) δ 6.83, 6.69 (2 br s, 4 H), 5.21 (s, 10 H), 2.71 (d, J = 6 Hz, 2 H), 0.22 (d, J = 6 Hz, 2 H); ^{1}H NMR (C_6D_6) δ 7.04 (s, 4 H), 4.57 (s, 10 H), 1.69 (s, 4 H); ^{13}C NMR ($CDCl_3$, 0 °C, undecoupled) δ 147.8 (s), 126.2 (d, J = 155 Hz), 124.2 (d, J = 160 Hz) (aromatic), 92.3 (d, J = 178 Hz, Cp), 6.7 (t, J = 139 Hz, CH_2). Anal. Calcd for $C_{20}H_{18}O_2Co_2$: C, 58.84; H, 4.44; Co, 28.87. Found: C, 58.68; H, 4.55; Co, 28.6.

Bis(μ-carbonyl)[bis(η^5-cyclopentadienyl)cobalt](*Co–Co*) (3). To a stirred suspension of 0.71 g of **2** (1.32 mmol) in 10 mL of THF was added 23 g of dry silica gel. The mixture immediately turned blue-green, indicative of the presence of **3**. After addition of 30 mL more of THF to the semisolid mixture, the reaction was allowed to stir for 1 h. The silica was filtered and washed with about 200 mL of benzene, until it was largely decolorized. After freezing the solution of **3** the solvent was removed by sublimation. The residue was then taken up in benzene and chromatographed on silica. Elution with benzene gave a small orange band of $CpCo(CO)_2$, followed by an intense blue-green band of **3**. A black-brown band characteristic of tri- and tetrameric CpCo carbonyl clusters was left at the top of the column. Removal of the benzene solvent again by sublimation gave 200 mg of **3** (50% yield) as an air-sensitive, analytically pure fine-crystalline blue-green material: mp >135 °C (slow decomposition); MS, *m/e* 304 (M$^+$), 276 (M$^+$ − CO); IR (benzene) 1790 (s) cm^{-1}; ^{1}H NMR (C_6D_6) δ 4.40 (s). Anal. Calcd for $C_{12}H_{10}O_2Co_2$: C, 47.40; H, 3.31. Found: C, 47.31; H, 3.55.

Sodium Bis(μ-carbonyl)bis[(η^5-methylcyclopentadienyl)cobaltate](*Co–Co*) (7). This compound was made by sodium amalgam reduction of $MeCpCo(CO)_2$ in a manner identical with that for preparation of **2**,[15] with one exception: dimethoxyethane (DME) rather than THF was used to extract the product **7** from the excess amalgam. The radical anion was obtained in 88% yield, containing about 10% (by weight) DME: IR (THF) 1736 (m), 1686 (m), 1653 (s) cm^{-1}.

Bis(μ-carbonyl)(μ-*o*-xylylene)bis[(η^5-methylcyclopentadienyl)cobalt](*Co–Co*) (8). A solution of 0.83 g of α,α'-dibromo-*o*-xylene (3.14 mmol) in 5 mL of THF was added dropwise, over 1 min, to 1.01 g of **7** (2.67 mmol) in 20 mL of THF. The mixture was allowed to stir for 2 min, during which time the color changed from the bright green of **7** to the olive-green of **8**. The solution was treated with 25 mL of hexane to precipitate NaBr and then chromatographed on a short column of alumina. Elution with hexane yielded a small red band, which was discarded, and then (still essentially with the solvent front) a large dark olive-green band. Further elution with benzene yielded another dark green band of **8**. The fractions were combined and the solvent removed in vacuo. Failure to immediately chromatograph the entire reaction mixture resulted in greatly reduced yields of **8**. The residue obtained was then rechromatographed on alumina, eluting with hexane to remove an orange-red band of $MeCpCo(CO)_2$ and then with benzene to yield a dark green fraction. This fraction was frozen and the solvent removed by sublimation to yield 250 mg (21% yield) of **8** as a dark green air-stable (as a solid) powder. Crystallization from methylene chloride/pentane at −40 °C gave analytically pure black-green rectangular crystals: mp 83.5–85 °C; IR (benzene) 1846 (w), 1806 (s) cm^{-1}; ^{1}H NMR (C_6D_6) δ 7.05 (s, 4 H), 4.44 (t, J = 2.1 Hz, 4 H), 4.32 (t, J = 2.0 Hz, 4 H), 1.77

(40) (a) Chetcuti, M. J.; Chisholm, M. H.; Folting, K.; Haitko, D. A.; Huffman, J. C. *J. Am. Chem. Soc.* **1982**, *104*, 2138–2146; (b) Halpern, J. *Inorg. Chim. Acta* **1982**, *62*, 31–37.

(41) Rausch, M. D.; Genetti, R. A. *J. Org. Chem.* **1970**, *35*, 3888–3897.

(42) See ref 14 for assignments.

(s, 6 H), 1.60 (s, 4 H); ^{1}H NMR (toluene-d_8, −90 °C) δ 4.34 (br s, 4 H), 4.23 (br s, 2 H), 4.11 (br s, 2 H), 2.46 (d, J = 6 Hz, 2 H), 1.79 (s, 6 H), 0.75 (d, J = 6 Hz, 2 H). Anal. Calcd for $C_{22}H_{22}O_2Co_2$: C, 60.57; H, 5.08. Found: C, 60.38; H, 5.07.

Although no attempt was made to isolate products from the reactions of **8**, IR and NMR evidence (including the low-temperature spectrum detailed above) indicated that the chemistry was analogous to that of **1**. In one experiment, a solution of **8** in C_6D_6 was warmed to 40 °C, resulting in 92% decomposition after 2 h at that temperature. Spectral analysis indicated that the products (formed in a 1:1 ratio) were $MeCpCo(CO)_2$ [IR (C_6D_6) 2016 (vs), 1956 (vs) cm^{-1}; ^{1}H NMR δ 4.54 (t, J = 2 Hz, 2 H), 4.35 (t, J = 2 Hz, 2 H), 1.39 (s, 3 H)] and MeCpCo(*o*-xylylene) [^{1}H NMR δ 7.27, 7.09 (AA′BB′), 4.69 (t, J = 2 Hz, 2 H), 3.95 (t, J = 2 Hz, 2 H), 2.52 (d, J = 2 Hz, 2 H), 1.44 (s, 3 H), −0.46 (d, J = 2 Hz, 2 H)]. In a second experiment, addition of one drop of PEt_3 to a benzene solution of **8** resulted in disappearance of the carbonyl band of **8** at 1806 cm^{-1} over the course of 10 min, with formation of a very strong band at 1743 cm^{-1} assigned to the dinuclear monophosphine adduct analogous to **20**.

(η^5-Cyclopentadienyl)(η^4-*o*-xylylene)cobalt (11). A suspension of 134 mg of **1** (0.33 mmol) in 20 mL of *n*-pentane was stirred at 35 °C for 3 days. Filtration of the dark red solution (yielding 10 mg of unreacted **1**) followed by removal of the solvent in vacuo gave a dark red solid. Sublimation for about 1 h at 32 °C and 0.002 mm gave 61 mg of **11** (88% yield based on recovered starting material) as slightly air-sensitive red-black crystals, leaving behind an oily red residue. Recrystallization from *n*-pentane at −40 °C gave analytically pure **11** as large, red-black needles: mp 63–64 °C; MS, m/e 228 (M$^+$); ^{1}H NMR (THF-d_8) δ 7.4, 7.2 (AA′BB′, 4 H), 4.49 (s, 5 H), 2.65 (d, J = 1.9 Hz, 2 H), −0.78 (d, J = 2.0 Hz, 2 H); ^{1}H NMR (C_6D_6) δ 7.35, 7.09 (AA′BB′, 4 H), 4.34 (s, 5 H), 2.65 (d, J = 1.4 Hz, 2 H), −0.54 (d, J = 1.4 Hz); ^{13}C NMR ($CDCl_3$, undecoupled) δ 135.0 (d, J = 158 Hz), 127.3 (d, J = 161 Hz) ("aromatic"), 92.1 (s, quaternary), 79.7 (d, J = 176 Hz, Cp), 26.1 (t, J = 156 Hz, CH_2). Anal. Calcd for $C_{13}H_{18}Co$: C, 68.43; H, 5.74; Co, 25.83. Found: C, 68.31; H, 5.68; Co, 25.7.

(η^4-1,3-Butadiene)(η^5-cyclopentadienyl)cobalt (12). Although syntheses of **12** have been claimed in the literature,[21] the only characterization has been a melting point (103–105 °C) reported by Pruett.[21a] We describe here a photolytic procedure for the preparation of **12** as well as complete analytical data. Thus, 0.51 g of $CpCo(CO)_2$ (2.63 mmol) in 7 mL of benzene was placed in a glass bomb equipped with a Teflon-brand vacuum stopcock, after which 5.2 mmol of butadiene were added by vacuum transfer. The reaction mixture was alternately irradiated and degassed, resulting in evolution of about 1.8 mmol of CO gas after 9 h of photolysis. In an attempt to drive the reaction further toward completion, an additional 5.7 mmol of butadiene was then transferred in. After 5 h of photolysis, only 0.1 mmol more of CO was evolved. The benzene was distilled from the deep red reaction mixture at room temperature under a pressure of 30 mm of nitrogen, giving a dark red oil. The residue was taken up in 2 mL of *n*-pentane and cooled to −40 °C to give 200 mg of fine red-black crystals; a second crop of 24 mg was subsequently obtained. The combined product was placed in a sublimation apparatus briefly at room temperature at 0.02 mm, allowing removal of $CpCo(CO)_2$ (**10**) to be followed. After washing a small amount of **10** off the cold finger, the product sublimed at 35 °C at 0.02 mm in 1 h, giving 200 mg of analytically pure **12** (43% yield) as slightly air-sensitive red-black crystals: mp 65–67 °C; MS, m/e 178 (M$^+$); ^{1}H NMR (C_6D_6) δ 4.91 (m, approximate d of t, J = 6.7, 2.0 Hz, 2 H), 4.58 (s, 5 H), 1.74 (approximate dd, J = 7.6, 1.5 Hz, 2 H), −0.32 (approximate dd, J = 8.5, 1.4 Hz, 2 H); ^{13}C NMR ($CDCl_3$, undecoupled) δ 79.5 (d, J = 175 Hz, Cp), 78.3 (d, J = 167 Hz, CH), 30.9 (t, J = 157 Hz, CH_2). Anal. Calcd for $C_9H_{11}Co$: C, 60.69; H, 6.23. Found: C, 60.58; H, 6.17.

Bis(μ-carbonyl)bis[(η^5-methylcyclopentadienyl)cobalt](*Co–Co*) (19). Treatment of 0.54 g of **7** (1.43 mmol) with silica and workup in a manner identical with that described above for the preparation of **3** gave 203 mg (43% yield) of **19** as an air-sensitive, analytically pure fine-crystalline blue-green solid: mp 110–112 °C dec; MS, m/e 332 (M$^+$); IR (benzene) 1784 (s) cm^{-1}; ^{1}H NMR (C_6D_6) δ 4.47 (t, J = 2.0 Hz, 4 H), 4.11 (t, J = 1.9 Hz, 4 H), 1.64 (s, 6 H). Anal. Calcd for $C_{14}H_{14}O_2Co_2$: C, 50.63; H, 4.25. Found: C, 50.39; H, 4.35.

Bis(μ-carbonyl)(dimethylphenylphosphine)bis[(η^5-methylcyclopentadienyl)cobalt](*Co–Co*) (20): A solution of 19 mg of $PPhMe_2$ (0.14 mmol) in 1 mL of benzene was added, dropwise, to a solution of 29 mg of **19** (0.09 mmol) in 3 mL of benzene. The color changed from blue-green to dark green and then to orange-brown as the phosphine addition was completed. The entire reaction mixture was immediately applied to an alumina column and washed with hexane, eluting excess phosphine and an orange band of $MeCpCo(CO)PPhMe_2$. The column was then washed with benzene, eluting a small orange band, which was discarded, and then a large bright green band. The solvent was removed from the green fraction by sublimation, leaving a black-green oily residue. This material was taken up in 1 mL of pentane and cooled to −40 °C to give 13 mg (30% yield) of **20** as air-stable, black crystals: mp 67–69 °C; MS, m/e 470 (M$^+$); IR (hexane) 1753 (s) cm^{-1}; ^{1}H NMR (C_6D_6)[42] δ 7.57 (m, 2 H), 7.06 (m, 3 H), 4.81 (s, 4 H), 4.49 (q, J = 2.0 Hz, 2 H), 4.15 (t, J = 1.6 Hz, 2 H), 2.09 (s, 3 H), 1.90 (br s, 3 H), 0.92 (d, J = 9.5 Hz, 6 H). Anal. Calcd for $C_{22}H_{25}O_2PCo_2$: C, 56.19; H, 5.36; P, 6.59. Found: C, 54.68; H, 5.48; P, 6.4.

Photolysis of 1. A 0.015 M solution of **1** was prepared by vacuum transfer of 1 mL of C_6D_6 onto 6 mg of **1** in an NMR tube, after which the tube was flame sealed under vacuum. Photolysis for 1 h gave a dark brown-red solution. The Cp region of the ^{1}H NMR had peaks at δ 4.68 (12%), 4.62 (14%), 4.64 (14%, $[CpCo(CO)]_3$), 4.57 (17%, **1**), 4.54 (7%), 4.48 (12%), 4.39 (13%, **10**), and 4.34 (11%, **11**). In addition to the doublets at δ −0.54 and 2.65 due to the endo and exo hydrogens of **11**, four roughly equally intense peaks, about two-thirds the height of those due to **11**, were observed at δ −1.40 (d, J = 2.7 Hz), −0.72 (d, J = 2.0 Hz), 1.81 (d, J = 1.5 Hz), and 2.49 (d, J = 2.2 Hz). The peaks at −1.40 and 2.49 disappeared upon continued irradiation. After 5 h, the Cp region showed peaks at δ 4.68 (3%), 4.62 (35%), 4.61 (18%, $[CpCo(CO)]_3$), 4.57 (4%, **1**), 4.54 (18%), 4.48 (9%), 4.39 (8%, **10**), and 4.34 (7%, **11**). The only additional significant changes observed upon letting the reaction mixture stand in the dark overnight were the disappearance of the δ 4.68 peak and an increase in the peak due to **10**. In addition to the bound *o*-xylylene peaks due to **11**, four sharply resolved signals that were clearly due to a single bound *o*-xylylene moiety were observed, at δ 5.60 (dd, J = 4.6, 2.5 Hz, 2 H), 2.70 (dd, J = 4.2, 2.8 Hz, 2 H), 1.81 (d, J = 1.5 Hz, 2 H), and −0.72 (d, J = 2.0 Hz, 2 H). The Cp singlet at δ 4.62 was apparently associated with these signals and integrated as 10 hydrogens. The signal at δ 4.68 could reasonably be assigned to the same compound as the bound *o*-xylylene doublets that had been observed at δ 2.5 and −1.4. We suggest that the major product is the bis π-allyl complex (μ-*o*-xylylene)bis(η^5-cyclopentadienyl)dicobalt, on the basis of the olefinic resonance at 5.60 and the two exo π-allylic resonances at 2.70 and 1.81. The remaining Cp peaks at δ 4.54 and 4.48 must be due to clusters that do not contain bound *o*-xylylene; on the basis of the observed Cp/CH_2 ratio, 35% of the *o*-xylylene was lost, presumably as its organic polymer. Finally, we note that attempts to scale up the reaction were unsuccessful.

Photolysis of 10 and 11. A sealed, evacuated NMR tube containing a 0.015 M solution of **1** in C_6D_6 was prepared as described above. The reaction mixture was heated at 43 °C for 2 h, effecting complete conversion to a 1:1 mixture of **10**/**11**. Irradiation for 2 h gave a mixture containing Cp peaks at δ 4.68 (2%), 4.62 (18%), 4.61 (9%, $[CpCo(CO)]_3$), 4.58 (7%, **1**), 4.54 (8%), 4.39 (19%, **10**), and 4.34 (37%, **11**). Further irradiation resulted in more decomposition of **10** and **11**, and increases in the peaks at δ 4.62 and 4.54. As with the photolysis of **1** itself, signals due to the same single major *o*-xylylene-containing compound were observed at δ 5.60, 2.70, 1.81, and −0.72, and the Cp/CH_2 ratio indicated a 21% loss of *o*-xylylene.

Carbonylation of 1: An NMR tube attached to a ground glass joint was charged with 20 mg of **1** (0.05 mmol) and then evacuated. Benzene-d_6 (0.5 mL) was then vacuum transferred into the tube, followed by 0.53 mmol carbon monoxide. The tube was sealed and heated to 35 °C for 5 min; at this temperature the calculated pressure was 6 atm. The dark green solution turned dark red; ^{1}H NMR showed a variety of aromatic, olefinic, and alkyl signals but only two Cp peaks, one at δ 4.57 (6%, **1**) the other at 4.39 (94%, **10**). The organic signals were the same as those due to *o*-xylylene dimers **14** and **15** (see below). Additional heating of the sample resulted in complete conversion of **1** to **10**; the integrated ratio of (**14** + **15**)/Cp_2 was 0.83:1.

Another, larger scale experiment was carried out with 60 mg of **1** (0.15 mmol) and 2.6 mmol of carbon monoxide (2 atm at room temperature) in benzene. Here, the color change seemed complete after 15 min. However, the organic products could not be separated from the organometallic product **10**.

Reaction of 1 and 1,2-Bis(diphenylphosphino)ethane (diphos). To a mixture of 40 mg of **1** (0.10 mmol) and 43 mg of diphos (0.11 mmol) was added 3 mL of THF. The reaction was allowed to stir for 30 min, during which time the color turned red, and monitoring by TLC showed that the starting material had disappeared. The solvent was removed in vacuo and the sticky red residue applied in benzene/hexane solution to an alumina column in the drybox. The column was washed with several column volumes of hexane to elute the *o*-xylylene dimers (fraction 1). Elution with benzene then yielded a bright orange fraction (2), and finally elution with THF yielded a third, dark orange fraction (3). Solvent removal from fraction 1 (on a rotary evaporator, in order not to lose the volatile products) yielded a small amount of short white needles (presumably **15**[27]) suspended in a colorless oil (presumably **14**[27]).

Table IV. Reaction Rate Constants for 1 → 17 (k_3), 17 → 2 16 (k_4) for PPh_3

$[PPh_3]^a$	$k_3 \times 10^4$, s^{-1} b	$k_{app} \times 10^4$, s^{-1} c	$k_4 \times 10^3$, s^{-1} d
0.010	3.12 ± 0.10	3.03 ± 0.14	2.1 ± 0.7
0.065	5.07 ± 0.14	4.32 ± 0.06	1.1 ± 0.1
0.21	6.24 ± 0.08	5.73 ± 0.08	2.5 ± 0.2
0.31	7.86 ± 0.10	7.10 ± 0.14	2.1 ± 0.2
0.48	9.36 ± 0.21	8.11 ± 0.40	1.9 ± 0.3
1.00	10.54 ± 0.28	9.52 ± 0.25	2.5 ± 0.3

[a] Moles per liter. [b] These values are actually the observed first-order rates diminished by the rates of formation of the thermal products 10 and 11. [c] These are the experimentally measured first-order rates of appearance of 16. [d] Determined as described in text.

Analysis by ^1H NMR indicated that the mixture contained only these two compounds in a 95:5 ratio of **14**/**15**. Addition of 4 μL of $CHCl_3$ as an internal NMR standard indicated that the yield of the two dimers was 5.6 mg (56%). **14**: ^1H NMR (CCl_4) δ 7.00 (s, 4 H), 6.08 (d, J = 9 Hz, 1 H), 5.78 (m, 3 H), 4.98 (d, J = 12.5 Hz, 2 H), 2.85 (approximate AB q, J = 15 Hz, 4 H), 1.91, 1.76 (m, 2 H), (lit.[27] δ 7.00, 5.8, 4.93, 2.8, 1.9). **15**: ^1H NMR (CCl_4) 6.88 (s, 8 H), 3.02 (s, 8 H), (lit.[27] δ 6.90, 3.03).

Solvent removal from fraction 2 yielded an orange powder presumed to be the symmetrical phosphine carbonyl complex $[CpCo(CO)]_2$(diphos): ^1H NMR (C_6D_6) δ 7.6 (m, 8 H), 6.95 (m, 12 H), 4.58 (s, 10 H), 2.82 (s, 4 H). Solvent removal from fraction 3 yielded a small amount of red oil, presumed to be the chelate bisphosphine complex CpCo(diphos): ^1H NMR (C_6D_6) δ 7.65 (m, 8 H), 6.95–7.1 (m, 12 H), 4.63 (s, 5 H), 1.81–1.88 (m, 4 H).

Carbonylation of 11. An NMR tube containing 10 mg of **11** (0.04 mmol), 0.53 mmol of carbon monoxide (6 atm) and 0.44 mL of C_6D_{12} was prepared in the same manner as that described above for the carbonylation of **1**. No reaction was detected as the sample was warmed to 70 °C, the only peaks present being due to **11** [^1H NMR δ 7.20, 7.04 (AA′BB′, 4 H), 4.28 (s, 5 H), 2.52 (d, J = 2.1 Hz, 2 H), −0.71 (d, J = 2.4 Hz, 2 H)]. Heating at 70 °C for 16 h resulted in the disappearance of 87% of **11**, with formation only of **10** (δ 4.82) and two new singlets of equivalent intensity at δ 7.04 and 3.26. Further heating resulted in complete conversion of **11** to **10** and the new organic product, identified as 2-indanone (**13**) by comparison to an authentic sample. The integrated ratio of **13**/**10** was 1.05:1.

Carbonylation of 12. An NMR tube containing 10 mg of **12** (0.06 mmol), 0.30 mmol of carbon monoxide (4 atmospheres at 70 °C), and 0.5 mL of C_6D_6 was prepared as described for the carbonylation of **1**. Heating from 30 to 55 °C for 2 h gave a low (2%) yield of **10**, and continued heating at 70 °C for 1 h gave a 10% yield of **10**. After a total of 18 h at 70 °C, 56% of the starting material had been converted to **10** and free butadiene, formed in a 1:1 ratio. Continued heating for 5 h to 120 °C led to 92% conversion of **12** to **10** and free butadiene; the integrated butadiene/**10** ratio was 0.94:1.

Kinetic Study of Reaction of 17 with Phosphines. Details of the experimental methods used in measuring these reaction rates by ^1H NMR may be found in the following paper.[14] For PMe_3, the rate of decrease of the sum of the integrated intensities of the two Cp peaks of **17** relative to the integrated intensity of the internal standard (ferrocene) was measured. For PPh_3, the rate of appearance of the Cp peak of the product $CpCo(CO)PPh_3$ (**16**), again relative to the ferrocene internal standard, was followed. At low values of $[PPh_3]$, the concentration of the intermediate **17** does not build up appreciably, resulting in similar rates of disappearance of **1** and appearance of **16**. In one case ($[PPh_3]$ = 0.03 M) the measured rate of appearance was actually slightly greater than that of disappearance, so this point was discarded. The rate data and derived values of k_4 are compiled in Table IV.

Crystal Structure of 8. Black, shiny, blade-like crystals were obtained by layering 4 mL of n-pentane onto 2 mL of a cold (−40 °C) saturated methylene chloride solution of 8 and allowing the mixture to remain undisturbed overnight at −40 °C. Although the crystals were apparently stable in air, fragments were mounted in thin-walled glass capillaries that were then flushed with dry nitrogen and flame sealed.

Preliminary precession photographs of several crystals yielded preliminary cell dimensions and revealed no symmetry higher than a center of inversion. A suitable fragment measuring 0.12 × 0.30 × 0.34 mm was then mounted on an Enraf-Nonius CAD-4 automatic diffractometer[43]

Table V. Crystal and Data Collection Parameters

compd	$Co_2C_{22}H_{22}O_2$ (8)	$CoC_{13}H_{18}$ (11)	$Co_2C_{22}H_{25}O_2P$ (20)
	Crystal Parameters at 25 °C[a]		
a, Å	9.1045 (11)	7.6286 (40)	10.0035 (14)
b, Å	9.5465 (13)	11.6094 (16)	14.0816 (13)
c, Å	11.8147 (16)	23.7196 (24)	14.4761 (18)
α, deg	83.730 (11)		
β, deg	81.414 (10)		92.042 (11)
γ, deg	63.392 (10)		
V, Å^3	906.8 (2)	2100.7 (8)	2037.9 (7)
space group	$P\bar{1}$ (No. 2)	$Pbca$ (No. 61)	$P2_1/c$ (No. 14)
M_r, amu	436.28	228.18	470.28
Z	2	8	4
d(calcd), g cm^{-3}	1.598	1.443	1.533
μ(calcd), cm^{-1}	18.39	15.85	17.2
size, mm	0.12 × 0.30 × 0.34	0.20 × 0.20 × 0.41	0.23 × 0.27 × 0.45
	Data Measurement Parameters		
diffractometer	Enraf-Nonius CAD-4		
radiation	Mo Kα ($\bar{\lambda}$ = 0.71073 Å)		
monochromator	highly oriented graphite ($2\theta_m$ = 12.2) perpendicular mode, assumed 50% perfect		
detector	crystal scintillation counter, with pulse-height analyzer		
aperture–crystal dist, mm	173		
vertical aperture, mm	3.0		
horizontal aperture, mm	2 + 1.0 tan (θ) (variable)		
reflections measured	$+h, \pm k, \pm l$	$+h, +k, +l$	$+h, +k, \pm l$
2θ range	3–45°		
scan type	θ–2θ		
scan speed (θ), deg/min	0.63–6.7	0.57–6.7	0.57–6.7
scan width ($\Delta\theta$)	0.5 + 0.347 tan θ	0.45 + 0.347 tan θ	0.45 + 0.347 tan θ
bkgd	0.25 ($\Delta\theta$) at each end of the scan		
reflections collecd	2553	1629	2972
unique reflections	2371	1370	2664
std reflections[b]	463, 5$\bar{1}$1, 018	(1,2,15), (521), (273)	$\bar{2}$39, 554, 293
orientation[c]	checked after every 250 measurements		

[a] Unit cell parameters and their esd's were derived by a least-squares fit to the setting angles of the unresolved Mo K$\bar{\alpha}$ components of 24 reflections with 2θ between 27° and 31° for 8, 27° and 28° for 11, and near 28° for 20. [b] Measured every 2 h of X-ray exposure time. Over the period of data collection no decay in intensity was observed. [c] Crystal orientation was redetermined if any of the 3 orientation check reflections was offset from its predicted position by more than 0.1°. Reorientation was not necessary during data collection.

and centered in the beam. Automatic peak search and indexing procedures yielded the same primitive cell obtained from the photographs. Inspection of the Niggli values[44] for the reduced primitive cell indicated no higher symmetry unit cells. The final cell parameters and pertinent details of the data collection procedure are given in Table V.

The 2553 raw intensity data were reduced to structure factor amplitudes and their esd's by correction for scan speed, background, and Lorentz and polarization effects.[45-47] Inspection of the azimuthal scan data[48] showed a minimum in the average relative intensity of 0.78. An absorption correction using a 12 × 6 × 12 Gaussian grid and the measured shape and size of the crystal was performed after the structure was solved but before refinement with anisotropic thermal parameters was carried out. The maximum and minimum transmission factors were 0.842 and 0.621, respectively.

After removal of redundant data ($0kl$, $k < 0$; $00l$, $l < 0$) the 2371 remaining unique data were used to form a Patterson synthesis that was solved for the Co positions in space group $P\bar{1}$ (No. 2). Standard Fourier and least-squares techniques located all other non-hydrogen atoms. The hydrogen atoms were located on the difference Fourier map following anisotropic refinement of all non-hydrogen atoms (R = 4.13%, wR = 7.07%).[49] All hydrogen atoms were allowed to refine freely and full-matrix least-squares refinement converged in four cycles (maximum $\Delta/\sigma \leq 0.35$ in the last cycle). The final residuals for 323 variables refined against the 2062 data for which $F^2 > 3\sigma(F^2)$ were R = 1.96%, wR = 2.98%, and GOF = 1.601. The R value for all 2371 data was 2.64%.

The quantity minimized by the least-squares program was $\sum w(|F_o| - |F_c|)^2$, where w is the weight of a given observation. The p factor,[49] used to reduce the weight of intense reflections, was set to 0.03 throughout the refinement. The analytical forms for the scattering factor tables for the neutral atoms were used[50] and all non-hydrogen scattering factors were corrected for both the real and imaginary components of anomalous dispersion.[51]

Inspection of the residuals ordered in ranges of sin θ/λ, $|F_o|$, and parity and value of the individual indexes showed no unusual features or trends. There was no evidence of secondary extinction in the low-angle, high-intensity data. The largest peak in the final difference Fourier map had an electron density of 0.16 $e^-/Å^3$ located near methyl carbon C(26). The positional and thermal parameters of the refined atoms and a listing of the values of F_o and F_c are available as supplementary material.

Crystal Structure of 11. Clear red columnar crystals of **11** were obtained by cooling a pentane solution to −40 °C overnight. Since the crystals decomposed slowly in air, suitable fragments were cleaved from the better shaped crystals and mounted in thin-walled glass capillaries, which were then flushed with dry nitrogen and flame sealed.

Preliminary precession photographs indicated orthorhombic symmetry and yielded rough cell dimensions. The data crystal, a roughly hexagonal prism measuring 0.20 × 0.20 × 0.41 mm, was then transferred to the diffractometer[43] and centered in the beam. Automatic peak search and indexing gave the same cell as preliminary camera work. Inspection of the primary zones revealed systematic absences for $0kl$, $k \neq 2n$; $h0l$, $l \neq 2n$; $hk0$, $h \neq 2n$ consistent only with space group $Pbca$ (No. 61). Final cell parameters and details of data collection are given in Table V.

The 1629 raw intensity data were reduced to structure factor amplitudes and their esd's as described above. Inspection of the azimuthal scan data showed only a ±2% nonsystematic variation of relative intensity. No absorption correction was performed.

Deletion of systematically absent reflections from the data set yielded 1370 unique reflections. The structures was solved from the Patterson map and refined via normal Fourier and least-squares methods (with anisotropic thermal parameters) to R = 5.0%, wR = 7.8%. A difference Fourier synthesis clearly showed the positions of all but one cyclopentadienyl hydrogen. All 13 hydrogen atoms were than included in least-squares refinement, with isotropic thermal parameters. In the last cycles an isotropic secondary extinction parameer[52] was included in the refinement.

The final residuals for 180 variables refined against the 1097 data for which $F^2 > 3\sigma(F^2)$ were R = 2.34%, wR = 3.08%, and GOF = 1.560. The R value for all 1370 data was 3.90%. The analytical and statistical forms used were the same as those described above for **8**. Inspection of the residuals ordered in ranges of sin θ/λ, $|F_o|$, and parity, and value of the individual indexes showed no unusual features or trends. The final value of the extinction parameter was $g = 3.7 \times 10^{-7}$, a 15% correction on the structure factor of the most intense reflection. The largest peak in the final difference Fourier map had an electron density of 0.21 $e^-/Å^3$, near the Co. The positional and thermal parameters of the refined atoms and listing of the values of F_o and F_c are available as supplementary material.

Crystal Structure of 20. Tabular shiny black crystals were obtained by slowly cooling an *n*-pentane solution of **20** to −40 °C. The crystals were mounted as for **8**. Preliminary precession photographs indicated Laue group $P2/m$ and yielded rough cell dimensions. The data crystal was then examined on the diffractometer[43] as described above for **8**. Inspection of $h0l$ and $0k0$ reflections showed systematic absences for $h0l$, $l \neq 2n$; $0k0$, $k \neq 2n$ consistent only with space group $P2_1/c$ (No. 14). Final cell dimensions and details of the data collection are given in Table V.

The 2972 raw intensity data were reduced to values of the structure factor amplitudes and their esd's as described above. Analysis of the azimuthal scan data showed an average I_{min}/I_{max} ratio of 0.86. An empirical absorption correction on the basis of the azimuthal scans was applied to the data because the crystal shape was not well-enough defined to allow a more analytical correction to be made.

Following removal of systematically absent and redundant data, the 2664 remaining data were used to calculate a Patterson synthesis, which yielded the positions of the two cobalt atoms and the phosphorus atom. Subsequent location and refinement of all other atoms proceeded normally. In the final cycles of least-squares refinement the hydrogen atoms were included in structure factor calculations in their idealized positions but were not refined. The final residuals for 244 variables refined against the 2385 data for which $F^2 > 3\sigma(F^2)$ were R = 2.21%, wR = 3.45%, and GOF = 1.85. The R value for all 2664 data was 2.76%. The analytical and statistical forms used were the same as those described above for **8**.

Inspection of the residuals ordered in ranges of sin θ/λ, F_o, and parity, and value of the individual indexes again showed no unusual features or

(43) Instrumentation at the University of California Chemistry Department X-ray Crystallographic Facility (CHEXRAY) consists of two Enraf-Nonius CAD-4 diffractometers, one controlled by a DEC PDP 8/a with an RKO5 disk and the other by a DEC 8/e with an RL01 disk. Both use Enraf-Nonius software as described in the CAD-4 Operation Manual, Enraf-Nonius, Delft, Nov. 1977, updated Jan. 1980.

(44) Roof, R. B., Jr., "A Theoretical Extension of the Reduced-Cell Concept in Crystallography"; Publication LA-4038, Los Alamos Scientific Laboratory: Los Alamos, NM, 1969.

(45) All calculations were performed on a PDP 11/60 equipped with 128 kilowords of memory, twin RK07 28 MByte disk drives, Versatec printer/plotter and TU10 tape drive using locally-modified Nonius-SDP[46] software operating under RSX-11M.

(46) Structure Determination Package User's Guide, April, 1980—Molecular Structure Corporation, College Station, TX 77840.

(47) The data reduction formulas are

$$F_o^2 = (\omega/\mathrm{Lp})(C - 2B) \qquad \sigma_o(F_o^2) = (\omega/\mathrm{Lp})(C + 4B)^{1/2}$$

$$F_o = (F_o^2)^{1/2} \qquad \sigma_o(F) = \sigma_o(F_o^2)/2F_o$$

where C is the total count in the scan, B the sum of the two background counts, ω the scan speed used in deg/min, and

$$\frac{1}{\mathrm{Lp}} = \frac{\sin 2\theta\,(1 + \cos^2 2\theta_m)}{1 + \cos^2 2\theta_m - \sin^2 2\theta}$$

the correction for Lorentz and polarization effects for a reflection with scattering angle 2θ and radiation monochromatized with a 50% perfect single-crystal monochrometer with scattering angle $2\theta_m$.

(48) Reflections used for azimuthal scans were located near $\chi = 90°$ and the intensities were measured at 10° increments of rotation of the crystal about the diffraction vector.

(49)

$$R = \frac{\sum||F_o| - |F_c||}{\sum|F_o|}$$

$$wR = \left[\frac{\sum w(|F_o| - |F_c|)^2}{\sum wF_o^2}\right]^{1/2}$$

$$\mathrm{GOF} = \left[\frac{\sum w(|F_o| - |F_c|)^2}{(n_o - n_v)}\right]^{1/2}$$

where n_o is the number of observations, n_v is the number of variable parameters, and the weights w were given by

$$w = 4F_o^2/\sigma^2(F_o^2) \qquad \sigma^2(F_o^2) = \sigma_o^2(F_o^2) + (pF^2)^2$$

where p is the factor used to lower the weight of intense reflections.

(50) Cromer, D. T.; Waber, J. T. "International Tables for X-ray Crystallography"; Kynoch Press: Birmingham, England, 1974; Vol. IV, Table 2.2B.

(51) Cromer, D. T., ref 50, Table 2.3.1.

(52) Zachariesen, W. H. *Acta. Crystallogr.* **1963**, *16*, 1139–1144.

trends. There was no evidence of secondary extinction in the low-angle, high-intensity data, save for one reflection (021) that seemed badly affected. Since other reflections of nearly the same intensity were not, no correction was performed. The largest peak in the final difference Fourier map had an electron density of 0.23 $e^-/Å^3$. The positional and thermal parameters for **20** and a listing of the values of F_o and F_c are available as supplementary material.

Acknowledgment. We are grateful to Professor H. Werner for communicating research results to us prior to publication and to a referee for a very thorough reading of the manuscript and a number of helpful suggestions (especially on nomenclature). Financial support for this work was provided by National Science Foundation Grant CHE79-26291. W.H.H. acknowledges an NIH National Research Service Award (F32-GM-07539) from the National Institute of General Medical Sciences. The crystal structure analyses were performed at the U. C. Berkeley X-ray Crystallographic Facility (CHEXRAY). Funds for the analyses were provided by the above NIH grant; partial funding for the equipment in the facility was provided by the NSF through Grant CHE79-07027. R.G.B. acknowledges a Research Professorship (1982-1983) from the Miller Institute for Basic Research at U. C. Berkeley.

Registry No. **1**, 79931-94-5; **2**, 62602-00-0; **3**, 58496-39-2; **7**, 86364-94-5; **8**, 86364-95-6; **10**, 12078-25-0; **11**, 79931-95-6; **12**, 1271-08-5; **13**, 615-13-4; **14**, 4968-91-6; **15**, 1460-59-9; **16**, 12203-85-9; **19**, 86364-96-7; **20**, 86364-97-8; $MeCpCo(CO)_2$, 75297-02-8; $MeCpCo(CO)PPhMe_2$, 86364-98-9; $[CpCo(CO)]_2$(diphos), 86365-00-6; CpCo(diphos), 86365-01-7; α,α'-dibromo-*o*-xylylene, 91-13-4; (μ-*o*-xylylene)bis(η^5-cyclopentadienyl)dicobalt, 86364-99-0.

Supplementary Material Available: For compounds **8**, **11**, and **20**, positional and thermal parameters and their estimated standard deviations, general temperature factor expressions, *B*'s, and listings of observed and calculated structure factors (38 pages). Ordering information is given on any current masthead page.

Kinetics and Mechanism of Decomposition of a Benzodicobaltacyclohexene: Reversible Dinuclear Elimination of *o*-Xylylene via a Dimetalla-Diels-Alder Reaction

William H. Hersh and Robert G. Bergman*

Contribution from the Department of Chemistry, University of California, Berkeley, California 94720. *Received December 27, 1982*

Abstract: A detailed mechanistic study of several reactions of the first dimetallacyclohexene, (η^5-Cp)$_2$Co$_2$(μ-CO)$_2$(μ-*o*-xylylene) (**1**), is described. The predominant reaction pathway is proposed to involve reversible cleavage of **1** in Diels-Alder fashion, into free *o*-xylylene (**3**) and the metal-metal double-bonded dimer **9**. Several lines of evidence support this conclusion. Crossover experiments demonstrated that loss of **3** from **1** in its reaction with $PPhMe_2$ to give dinuclear monophosphine adduct **2** is a dinuclear elimination process that leaves the cobalt-cobalt bond intact. Kinetic studies showed that sufficiently high concentrations of several ligands (phosphines, bis(methylcyclopentadienyl) metal-metal double-bonded dimer **10**, or dimethyl acetylenedicarboxylate (DMAD)) induce decomposition of **1** at the same maximum rate, to give monophosphine adduct **2**, bis(methylcyclopentadienyl) dimetallacyclohexene **5**, or dinuclear DMAD adduct **16**, respectively. Both the phosphine and DMAD reactions exhibited falloff in the observed rates of decomposition at lower ligand concentration. On the basis of the proposal that **1** was in thermal equilibrium with two reactive intermediates (**3** and **9**), theoretical results suggested, and were experimentally confirmed, that at low DMAD concentration the falloff in decomposition rate could be eliminated by lowering the concentration of **1**, to again induce decomposition at the previously observed maximum rate. An Arrhenius plot of data collected in this limiting rate regime, representing the rate of the retro-dimetalla-Diels-Alder reaction, gave $\Delta H^{\ddagger} = 24.3$ kcal/mol and $\Delta S^{\ddagger} = +12.1$ eu. Preparative reactions of double-bonded dimer **9** with two different *o*-xylylene precursors gave moderate yields of metallacycle **1**, providing additional evidence for the forward dimetalla-Diels-Alder reaction. A minor reaction pathway, thermal decomposition of **1** to CpCo(*o*-xylylene) (**12**) and $CpCo(CO)_2$ (**13**), was also observed. Evidence is presented suggesting that it is mechanistically related to the major decomposition pathway operating in other dinuclear dicobalt systems, involving intramolecular alkyl to cobalt migration.

The recent surge in interest in the chemistry of transition-metal cluster compounds has been fueled by the notion that the behavior of these materials may model that found at metal surfaces.[1] One reason for wanting to model surface reactions is that certain heterogeneous reactions, such as the Fischer-Tropsch reaction and C-H and C-C bond activation, have so far been duplicated only rarely in solution.[2-4] Since a reason for this difficulty may be that more than one metal center in some cases is needed to effect such reactions, metal clusters are obvious candidates for

Scheme I

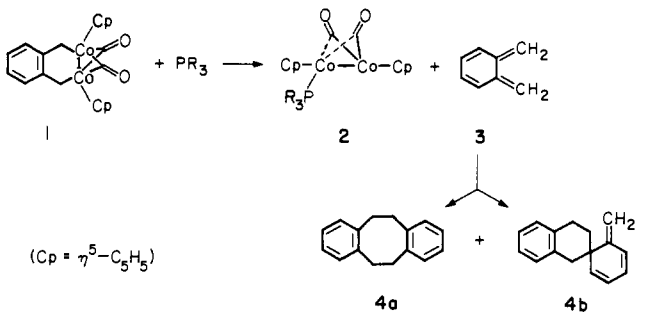

(1) (a) Muetterties, E. L. *Bull. Soc. Chim. Belg.* **1975**, *84*, 959-986. (b) Lewis, J.; Johnson, B. F. G. *Pure Appl. Chem.* **1975**, *44*, 43-79. (c) Muetterties E. L.; Stein, J. *Chem. Rev.* **1979**, *79*, 479-490.

(2) For homogeneous Fischer-Tropsch reactions, see: (a) Thomas, M. G.; Beier, B. F.; Muetterties, E. L. *J. Am. Chem. Soc.* **1976**, *98*, 1296-1297. (b) Demitras, G. C.; Muetterties, E. L. *Ibid.* **1977**, *99*, 2796-2797. (c) Perkins, P.; Vollhardt, K. P. C. *Ibid.* **1979**, *101*, 3985-3987. (d) For a demonstration that a system thought to display Fischer-Tropsch chemistry in fact does not, see: Benner, L. S.; Lai, Y. H.; Vollhardt, K. P. C. *Ibid.* **1981**, *103*, 3609-3611.

0002-7863/83/1505-5846$01.50/0